http://multires.caltech.edu/pubs/sqrt3.pdf (submitted for publication)

Composite Primal/Dual $\sqrt{3}$-Subdivision Schemes

Peter Oswald
Bell Labs

Peter Schröder
Caltech

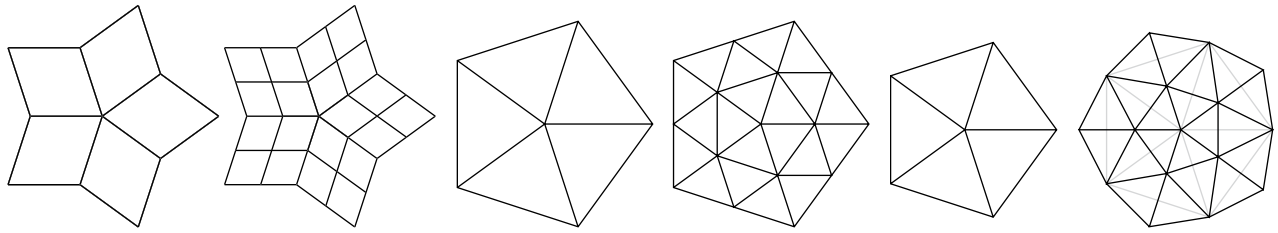
Abstract

We present new families of primal and dual subdivision schemes for triangle meshes and $\sqrt{3}$-refinement. The proposed schemes use two simple local rules which cycle between primal and dual meshes a number of times. The resulting surfaces become very smooth at regular vertices if the number of cycles is ≥ 2. The C^1-property is violated only at low-valence irregular vertices, and can be restored by slight modifications of the local rules used.

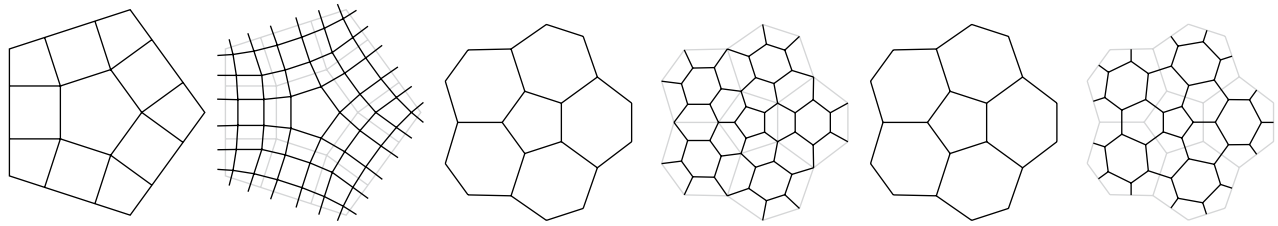
As a generalization, we introduce a wide class of composite subdivision schemes suitable for arbitrary topologies and refinement rules. A composite scheme is defined by a simple upsampling from the coarse to a refined topology, embedded into a cascade of geometric averaging operators acting on coarse and/or refined topologies. We propose a small set of such averaging rules (and some of their parametric extensions) which allow for the switching between control nets associated with the same or different topologic elements (vertices, edges, faces), and show a number of examples, based on triangles, that the resulting class of composite subdivision schemes contains new and old, primal and dual schemes for $\sqrt{3}$-refinement as well as for quadrisection. As a common observation from the examples considered, we found that irregular vertex treatment is necessary only at vertices of low valence, and can easily be implemented by using generic modifications of some elementary averaging rules.

1 Introduction

Subdivision schemes for arbitrary topology surfaces can be broadly classified according to their topologic and geometric refinement rules. For example, the schemes of Catmull-Clark [1]—for quadrilateral control meshes—and of Loop [9]—for triangle control meshes—are based on *topologic quadrisection* of faces (Figures 1(a) and 1(b)) and use repeated averaging as their geometric rule. Since they split faces they are *primal* schemes. In contrast, *dual* schemes split vertices (Figures 1(d) and 1(e)). The Doo-Sabin scheme [2], for example, is a dual quadrilateral scheme (Figure 1(d)), while half box splines [10]—being dual triangle schemes based on vertex quadrisection—lead to hexagonal tilings (Figure 1(e)).



(a) Primal quadrilateral quadrisection. (b) Primal triangle quadrisection. (c) Primal $\sqrt{3}$ (trisection) subdivision.



(d) Dual quadrilateral quadrisection. (e) Dual triangle quadrisection. (f) Dual $\sqrt{3}$ (trisection) subdivision.

Figure 1: *Topologic styles of subdivision. For each pair the coarser level is shown on the left with the finer level on the right.*

Given these basic schemes one may ask for interrelationships between them both in terms of geometric and topologic rules. In the case of univariate splines, for example, the Lane-Riesenfeld algorithm [8] establishes an interlaced ladder of increasing

order B-splines through repeated averaging. Here a single geometric rule, which averages back and forth between primal and dual meshes after upsampling, generates B-splines of arbitrary order. For quadrilateral schemes this relationship continues to hold in the arbitrary topology setting, as recently established by Zorin and Schröder [17] and Stam [12].

Even more interesting are schemes in which the topologic subdivision rule calls for *joining* primal and dual meshes in some fashion. An example are the primal $\sqrt{3}$-schemes [3, 6, 7] in which the refined mesh contains all vertices of the primal and dual mesh (Figure 1(c)). The first examples of $\sqrt{3}$-schemes used geometric rules which were constructed in an adhoc manner. Dual schemes of this type are possible as well (Figure 1(f)) but have not yet been considered.

The motivation for the present paper was the desire to find a set of simple ("atomic") rules which could be composed to produce families of primal and dual $\sqrt{3}$-schemes of increasing smoothness, mimicking the state of affairs in the construction of primal and dual quadrilateral quadrisection schemes. Indeed, such constructions are possible, and we introduce them here. While these constructions can recover some known schemes we will focus more on repeated averaging as a basic tool for new schemes and future explorations. Consequently we will not explore interpolatory schemes or consider boundaries. Examples of the former are explored in [7, 5] while the latter may be addressed in standard ways (see for example Kobbelt [6]).

In Section 2.1, we consider the particular family $VFV(n)$ of primal $\sqrt{3}$-subdivision schemes in which trivial upsampling to the refined control mesh is followed by n cycles of applying vertex-to-face (or VF) and face-to-vertex (or FV) averaging rules. The underlying theory and smoothness analysis for $VFV(n)$ in the regular setting are described in a companion paper by Jiang and Oswald [4]. Here we focus on the investigation of the smoothness of subdivision surfaces generated by these schemes near irregular points (irregular vertices in primal schemes; irregular faces in dual schemes) in the arbitrary topology setting. It turns out that only low valence irregular points may cause loss of C^1-smoothness, and that simple modifications of the averaging rules correct the situation (Section 2.1.3). In Section 2.2 the associated dual schemes $FVF(n)$ are defined by FV-averaging on the coarse mesh, followed by $VFV(n-1)$ and another VF-averaging on the refined mesh. These inherit their properties from $VFV(n)$ in a straightforward manner.

These results lead to the natural question whether one can use the idea of building schemes from a fixed set of elementary averaging rules for triangle schemes—and their modifications near irregular points—in a broader context. The appeal of such an approach is conceptual simplicity and generality: the same geometric rules can be applied equally to different topologic refinement rules encompassing trisection ($\sqrt{3}$-subdivision schemes) and quadrisection of both primal and dual types.

In Section 3, we propose a small list of elementary averaging rules associated with vertex (V), edge (E), and face (F) entities for primal (triangle) and dual (hexagon) control meshes, and demonstrate that building composite subdivision schemes from them covers a number of known schemes, such as Kobbelt's $\sqrt{3}$-subdivision scheme or Loop's scheme as well as new families of potentially attractive schemes. A consequence of recovering, for example, Kobbelt's $\sqrt{3}$ scheme as a sequence of repeated primal/dual averaging steps is that we can immediately give an associated dual $\sqrt{3}$ scheme with the *same* smoothness properties as the original Kobbelt scheme. A common observation is that the C^1 behavior is jeopardized only for irregular points of low valence, and that simple modifications of the averaging rules, similar to those proposed for $VFV(n)$, also helped in all other examples we considered.

2 Repeated Averaging Operators for $\sqrt{3}$-Subdivision

We begin with a discussion of primal schemes. Dual schemes follow almost trivially from these and will be briefly discussed at the end of this section. For purposes of exposition we relegate technical details of the eigen value analysis, upon which our claims are based, to the Appendices.

2.1 Primal $VFV(n)$ Schemes

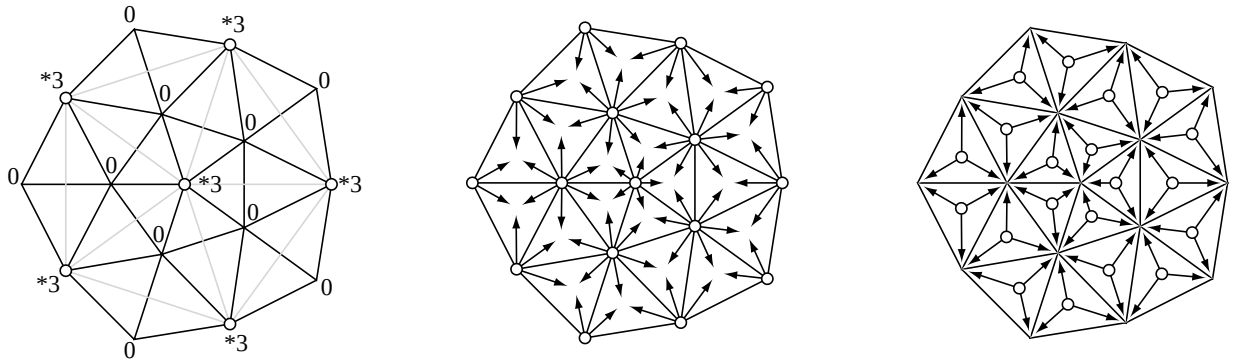
We motivate our repeated primal/dual averaging constructions with a very simple interpolating primal $\sqrt{3}$-subdivision scheme. It assigns each new vertex in the finer mesh a control point which is the average of the three control points associated with the incident vertices in the coarser mesh (Figure 2). New control points for the old vertices in the finer mesh are simply copies of their values in the coarser mesh, hence the construction is interpolating. This scheme corresponds to piecewise linear interpolation for $\sqrt{3}$-meshes. Instead of the usual line singularities for hat functions we have a point singularity due to the rotational "smearing" occurring in the $\sqrt{3}$-refinement process. While the resulting basis functions are thus less Hölder regular and may not be visually appealing, interestingly they have a somewhat higher Sobolev smoothness of 1.6571 versus 1.5 for the hat function [4].

The same scheme can also be constructed through upsampling followed by one primal-to-dual and one dual-to-primal averaging step (Figure 3). The upsampling step writes the old vertex values (multiplied by 3) to the corresponding vertices in the finer mesh. All new vertices at the finer level are initialized with the value 0 (Figure 3(a)). The first averaging step at the finer level computes face values as centroids of incident vertices (Figure 3(b)). In the second averaging step vertex values are computed as centroids of their incident face values. (Figure 3(c)). This sequence of steps reproduces the original control points at the vertices inherited from the coarser mesh while computing centroid averages at the finer mesh vertices corresponding to



Figure 2: *The simplest primal $\sqrt{3}$-subdivision scheme computes new control points which correspond to faces on the coarser level by averaging all incident triangle vertex control points (left). Control points for vertices inherited from the coarser mesh are copies of control points from the old mesh. Because of the latter the resulting scheme is interpolating. Examples of basis functions in the regular respectively irregular (valence 9) setting are shown on the right.*

the faces of the coarser mesh, as in the scheme above. The averaging process may now be repeated at the finer level using



(a) Upsampling multiplies old values by 3 and writes 0s to all new slots.

(b) The VF step centroid averages primal (vertex) quantities into dual (face) quantities.

(c) The FV step centroid averages dual (face) quantities into primal (vertex) quantities.

Figure 3: *Basic upsampling and averaging operators for the construction of $VFV(n)$ schemes.*

additional VF (primal to dual) and FV (dual to primal) centroid averaging steps, producing a hierarchy of subdivision rules

$$VFV(n) = (FV \circ VF)^n \circ T_{VV,3} \ , \qquad n \geq 1 \ ,$$

where $T_{VV,3}$ denotes the upsampling operator. All other operations are carried out on the fine triangulation. Note that only the $T_{VV,3}$ copying step depends on the refinement type. Obviously, $VFV(1)$ is the linear $\sqrt{3}$-subdivision rule.

2.1.1 Properties of $VFV(n)$ Schemes in the Regular Setting

In the regular setting, these schemes have been analyzed in [4, Section 3.3]. For the convenience of the reader, we recall the main results. Due to the construction of the subdivision rule $VFV(n)$ from repeatedly used elementary averaging steps, the symbol $P_{VFV(n)}(z)$ associated with the subdivision rule $VFV(n)$ automatically possesses a simple factorization

$$P_{VFV(n)}(z) = P(z)^n \ , \qquad n = 1, 2, \ldots ,$$

where $z = (z_1, z_2) = (e^{-it_1}, e^{-it_2})$, and

$$P(z) = \frac{1}{9}(3 + z_1 + \frac{1}{z_1} + z_2 + \frac{1}{z_2} + \frac{z_1}{z_2} + \frac{z_2}{z_1})$$

coincides with the symbol of the linear subdivision rule. Note that $P(z) \geq 0$ for all (t_1, t_2), and that it satisfies sum rules of order 2 (as is clear from the fact that the linear subdivision rule reproduces linear polynomials). Thus, the subdivision rule $VFV(n)$ reproduces polynomials of degree $2n - 1$, and determining its Sobolev and Hölder smoothness exponents becomes a relatively straightforward task. For $n \leq 4$, the results from [4] are summarized in Table 1. It is conjectured that similar results

Property	$n=1$	$n=2$	$n=3$	$n=4$
Sum rule order	2	4	6	8
Stability	yes	yes	yes	yes
Sobolev regularity	1.6571	3.9518	5.9960	7.9997
Hölder regularity	0.7381	3.3143	5.7073	7.9036

Table 1: *Basic properties of $VFV(n)$, $n \leq 4$, in the regular case*

hold for $n > 4$. In particular, $VFV(n)$ remains stable for all n, and Sobolev and Hölder exponents seem to approach very quickly their trivial upper bound $2n$ given by the sum rule order of the scheme. That the smoothness of the basis functions in the regular setting indeed rapidly increases with n is visualized in Figure 4.

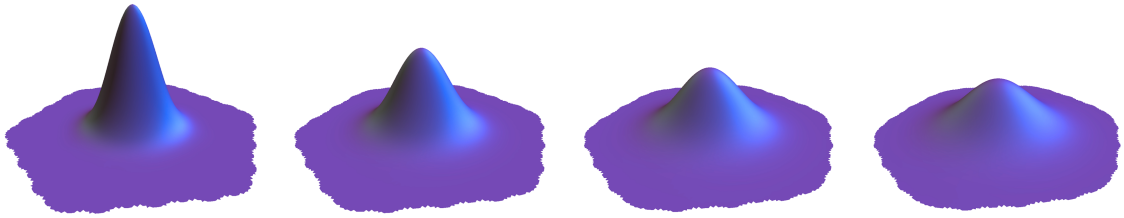
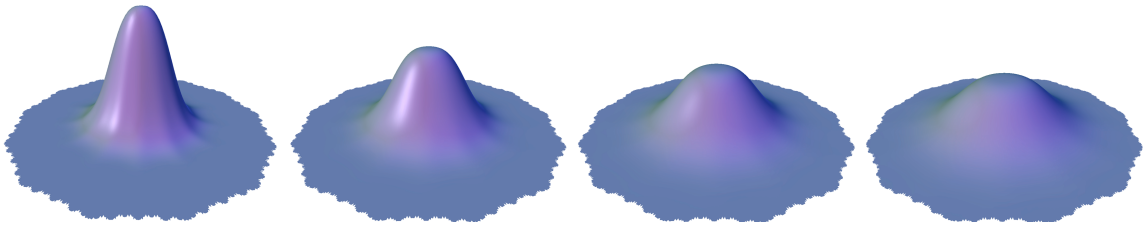


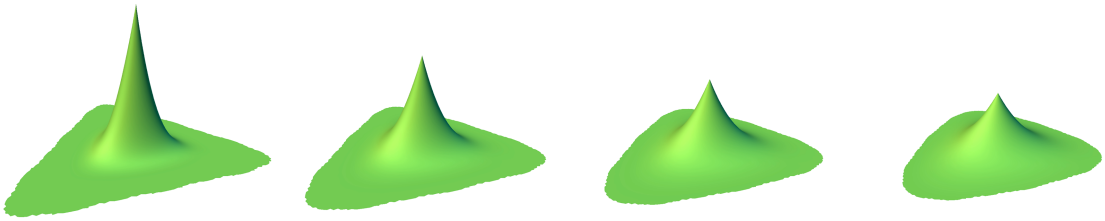
Figure 4: *Regular basis functions for $VFV(2)$ through $VFV(5)$ (left to right).*

2.1.2 Generalization to the Irregular Setting

It is clear that both VF and FV averaging rules are well defined in the arbitrary topology setting and can be readily applied to irregular connectivity control meshes. In fact, control meshes do not even need to consist of triangles for this method to work. Thus, the $VFV(n)$-schemes carry over automatically. From now on, we will concentrate on the regularity of these schemes near irregular vertices in the case $n \geq 2$, since the linear subdivision rule is not C^1 smooth even in the regular setting. While the direct application of $VFV(n)$ seems to work well near high valence vertices, it breaks down for vertices of valence $k = 3, 4$ (Figure 5).



(a) Basis functions for $k = 13$.



(b) Basis functions for $k = 3$.

Figure 5: *Irregular basis functions for $VFV(2)$ through $VFV(5)$ (left to right).*

The problem for low valences can be understood by considering the eigen structure of the subdivision operator around irregular vertices. We follow [11, 16] (although there the details are carried out for quadrisection, the basic methodology

remains the same for $\sqrt{3}$-subdivision), but leave out some technical steps. According to [16], in order to establish C^1 regularity of surfaces generated by a subdivision scheme S around a vertex of valence $k \geq 3$, we have to find the appropriate *invariant neighborhood* $N(S,k)$ in a k-regular triangulation, derive the *linear subdivision matrix* $\tilde{S}$ associated with $N(S,k)$, determine if there exists a so-called *dominant pair of cyclic eigen spaces* for $\tilde{S}$, and prove regularity and injectivity of the *characteristic map* of this pair in a neighborhood of the irregular vertex. A particularly simple but typical situation is that the relevant eigen values of $\tilde{S}$, counted with their multiplicities and ordered by decreasing magnitude, satisfy

$$\lambda_1 = 1 > |\lambda_2| = |\lambda_3| > |\lambda_4| \geq \dots \qquad (\lambda_2 \lambda_3 > 0).$$

Note that $\lambda_1 = 1 > |\lambda_2|$ is a necessary condition for the convergence of any subdivision scheme. If the subdivision rule is real-valued, local, and geometrically invariant, then the invariant neighborhood $N(S,k)$ can be chosen finite, and $\tilde{S}$ can be unitarily transformed into block-diagonal form. These facts allow us to simplify the underlying eigen value problem considerably. Assuming the above properties of the spectrum of $\tilde{S}$, a dominant pair of eigen spaces exists, and its associated characteristic map is given by

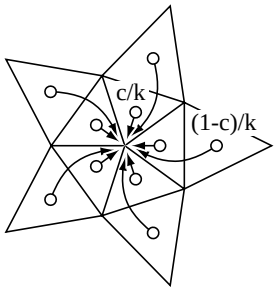
$$\Phi : \quad U_1 \longrightarrow (f_1, f_2) ,$$

where U_1 collects all triangles in the 1-ring around the irregular vertex. The real-valued functions f_l, $l = 1, 2$, are constructed as limit functions of the subdivision scheme with initial values obtained from the eigen spaces for λ_2, λ_3. Note that in these auxiliary constructions only those eigen values λ and eigen spaces of $\tilde{S}$ are taken into account for which the associated f does not vanish in a neighborhood of the irregular vertex. We refer to [16] for the detailed description of these issues.

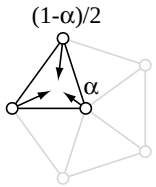
For $VFV(2)$ we find that the subdominant eigen values are complex conjugates, and found in blocks B_1 and B_{k-1} of the block-Fourier transformed $\tilde{S}$ (all the details are given in Appendix A.1). For $k = 3$ these eigen values are of magnitude $1/3$. Unfortunately, there is an eigen value $1/3$ in the block B_0 (which does not depend on k). Hence for $k = 3$, C^1 smoothness is lost. For $k = 4$ the formal conditions are met, but numerically the ratio of the subdominant eigen values and the eigen value $1/3$ in block B_0 is too close to 1 to be satisfactory. Luckily this situation can be remedied easily, and we now turn to two possible modifications.

2.1.3 Modifications for Irregular Vertices of Low Valence

To overcome the unsatisfactory behavior of $VFV(n)$ near irregular vertices for low valences, we propose two different modifications which preserve the basic structure of the above construction as much as possible. The first modifies the FV rule ("flap modification") while the second modifies the VF rule ("weight modification").



(a) Flap modification FV_c at an irregular vertex as a function of the parameter c.



(b) Weight modification $\widetilde{VF}_\alpha$ near an irregular vertex as a function of the parameter α.

Figure 6: *Modifications for irregular vertices of low valence.*

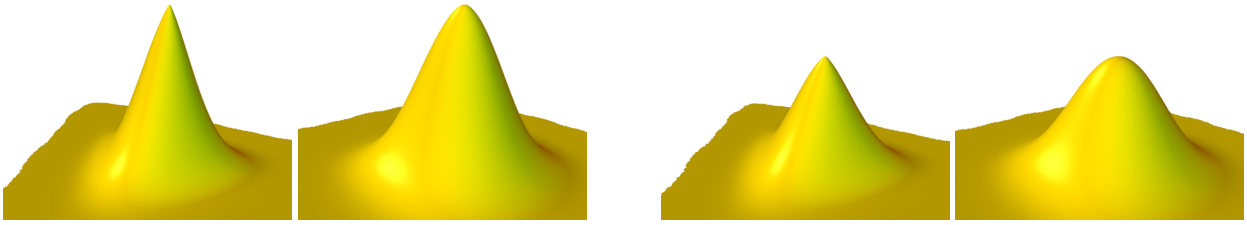
Flap modification applies to the FV rule. Instead of computing a vertex value as the centroid average of only its incident face values we also bring in the face values of the flaps, i.e., the faces which are edge adjacent to the first ring of triangles around the irregular vertex (Figure 6(a)).

There are several ways to use the flap rule FV_c as a building block for modifying $VFV(n)$. Set $VFV_c = FV_c \circ VF$, where the parameter c may depend on the valence k but is always $c = 1$ for $k = 6$. We consider

$$VFV_c(n) = (VFV_c)^n \circ T_{VV,3} , \quad VFV_{c,1}(n) = (FV \circ VF)^{n-1} \circ VFV_c \circ T_{VV,3} , \quad VFV_{c,n}(n) = VFV_c \circ VFV(n-1) .$$

The last two modifications are in some sense more economic since they require the flap rule only once per subdivision step. In Appendix A.2 we analyze the effect of the most general $VFV(2)$-replacement, $VFV_{c_1,c_2} = VFV_{c_2} \circ VFV_{c_1} \circ T_{VV,3}$, on the

subdivision operator S. As it turns out only the B_0 block changes and its troublesome eigen value $1/3$ will be decreased for *any* choice $0 \le c_1, c_2 \le 1$, $(c_1, c_2) \neq (1, 1)$ (see the discussion in Appendix A.2 and Figure 7(a)).



(a) Flap modification for $k = 3, 4$ with $c_1 = c_2 = .5$

(b) Weight modification for $k = 3, 4$ with $\alpha_2 = -1/3$.

Figure 7: *Effect of modifications to $VFV(2)$ on the basis functions at a $3, 4$-valent vertex (compare to 5(b)).*

Weight modification applies to the VF averaging rule by assigning arbitrary weights a_j to each incident vertex v_j of a triangle face such that the condition $a_1 + a_2 + a_3 = 1$ is observed. For example, if the valences of the three vertices v_1, v_2, v_3 are denoted by k_1, k_2, k_3, we could set

$$a_j = \frac{\tilde{k}_j}{\tilde{k}_1 + \tilde{k}_2 + \tilde{k}_3} , \quad \tilde{k}_j = \min(k_j, 6) , \qquad j = 1, 2, 3 .$$

In particular, if we have an isolated vertex $v = v_1$ of valence $k < 6$ ($k_1 = k$, $k_2 = k_3 = 6$) we get the weights

$$\alpha \equiv a_1 = k/(k + 12); \quad a_2 = a_3 = 6/(k + 12) ,$$

i.e., $\alpha = 1/5, 1/4, 5/17 < 1/3$ for $k = 3, 4, 5$, while for $k \ge 6$ we have the original VF rule. Such a weight modification which turns on only for low-valence vertices seems plausible since $VFV(n)$ works well in the high valence case.

This proposal is analyzed in Appendix A.3 by considering the general weight modification $\widetilde{VF}_\alpha$ for triangles with one irregular vertex (at v_1) and setting

$$a_1 = \alpha , \quad a_2 = a_3 = (1 - \alpha)/2 ,$$

see Figure 6(b). If v_1 is regular, i.e., all three vertices have valence 6, we insist on $\alpha = 1/3$. In analogy to the flap modifications, we could now define modified rules such as $VFV_\alpha(n)$ etc. by replacing VF by $\widetilde{VF}_\alpha$ accordingly. As before, we concentrate on $n = 2$, and consider the general VFV_{α_1,α_2} scheme. It turns out that we must have $\alpha_1 = 1/3$ to obtain meaningful results, leaving only the $VFV_{\alpha,n}(n)$ scheme, for which any $\alpha < 1/3$ yields the desired C^1-property. In practice, we use specific (sometimes negative) α values to achieve best visual results (see Appendix A.3, and Figure 7(b)).

2.2 Dual $FVF(n)$ Schemes

Since dual subdivision schemes assign control points to the faces of the mesh, the definition of $VFV(n)$ suggests the following definition of an associated $FVF(n)$ family of dual schemes:

$$FVF(n) = VF \circ VFV(n-1) \circ FV = (VF \circ FV)^{n-1} \circ VF \circ T_{VV,3} \circ FV .$$

I.e., these schemes execute a dual to primal averaging step on the coarse mesh, a trivial upsampling step to the fine mesh and a primal to dual averaging step on the fine mesh followed by $n - 1$ rounds of $FVF = VF \circ FV$ averaging. Any modifications near low-valence vertices can be incorporated as before, with the similar restriction that no weight modification $\widetilde{VF}_\alpha$ is allowed directly after $T_{VV,3}$.

There is no need to perform additional smoothness analysis: the associated $FVF(n)$ schemes behave similar to $VFV(n)$ in almost all respects. The basis function of a $FVF(n)$ scheme corresponding to a particular face is a linear combination of the basis functions of the $VFV(n)$ scheme for its vertices, thus smoothness properties are inherited. On the downside, this implies slightly less local behavior and more linear dependencies between the $FVF(n)$ basis functions. See Appendix A.4 for more details. Figure 9 shows examples of the resulting basis functions in the regular and irregular setting, while Figures 10 and 11 show the results of dual subdivision ($FVF(2)$) applied to more complex meshes.

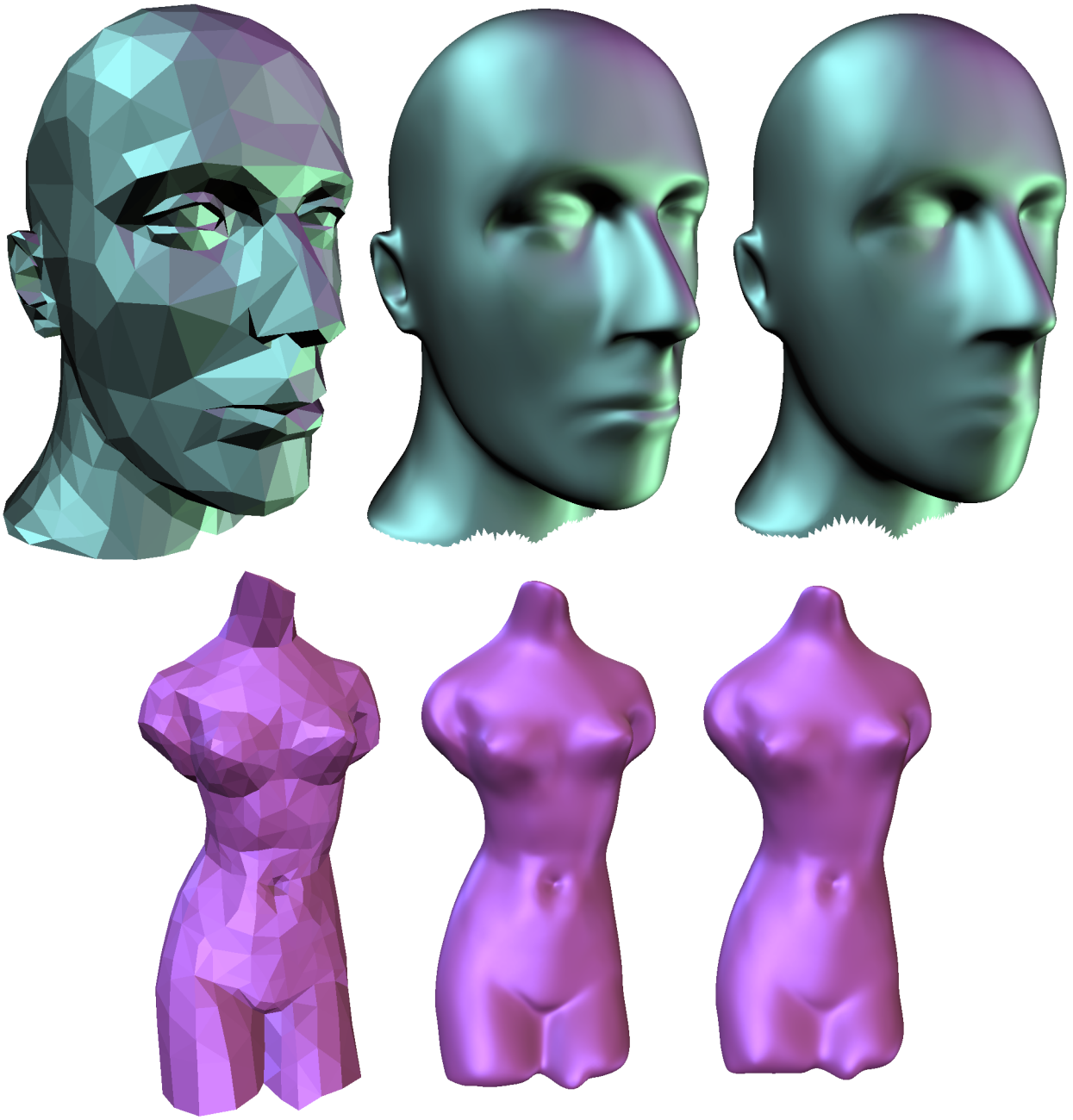


Figure 8: *Examples of $VFV(2)$ and $VFV(4)$ subdivision (with weight modification for $k = 3, 4$) for the mannequin and venus models with the respective control meshes on the left.*

3 Composite Vertex/Edge/Face Schemes

In this section, we initiate a broader discussion of the repeated use of what we call *elementary averaging rules* involving different topologic elements (vertices, edges, faces) for custom building primal/dual triangle based subdivision schemes. Several observations motivate such an undertaking:

- Some of the most attractive subdivision schemes are of this type (e.g., quadrilateral schemes [17, 14]). Here we enlarge this set to include a number of different triangle based schemes.
- Averaging rules are simple to implement on general topologies. They do not need the setup of complicated local stencils. Instead local stencils are the result of cascading very simple schemes.
- The same rules can be used to build primal and dual subdivision schemes associated with different refinement patterns such

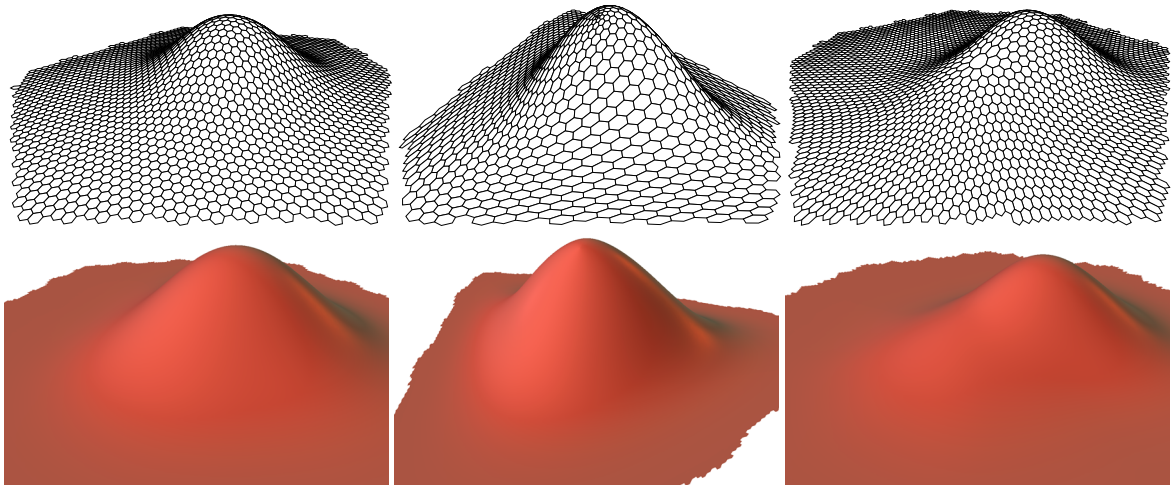


Figure 9: *Basis functions of dual $\sqrt{3}$-schemes based on $FVF(2)$ repeated averaging (with weight modification) for $k = 6, 3, 9$.*

as quadrisection (both triangles and quadrilaterals), $\sqrt{3}$-triangle, and $\sqrt{2}$-quadrilateral refinement.

- Higher regularity is easy to achieve by investing more elementary steps per subdivision step.
- As we demonstrated for $VFV(n)$, necessary enhancements near irregular vertices can be implemented by slightly modifying elementary rules. Averaging schemes tend to automatically treat high valence vertices well, leaving problems only for low-valence vertices.
- The analysis of such schemes in the regular case benefits from compact representations of symbols and symbol factorizations.

We begin by introducing some useful language for this discussion. For simplicity, we will stick with the bivariate setting, where the topology is represented by vertices (V) of valence $k \geq 3$, edges connecting two vertices (E), and faces (F) of valence l, i.e., triangles ($l = 3$), quadrilaterals ($l = 4$), hexagons ($l = 6$), etc. We call these *topologic elements*. We also need neighbor relations between topologic elements. For the purpose of this discussion, we assume the following standard *primary neighbor relations* and indicate the associated averaging operators (Figure 12):

1. vertices incident to a face, $f \longmapsto V(f) = \{v_1, v_2, v_3, \ldots, v_l\}$ (Figure 12(a));
2. edges incident to a face, $f \longmapsto E(f) = \{e_1, e_2, e_3, \ldots, e_l\}$ (Figure 12(b));
3. faces incident to a vertex, $v \longmapsto F(v) = \{f_1, f_2, f_3, \ldots, f_k\}$ (Figure 12(c));
4. edges incident to a vertex, $v \longmapsto E(v) = \{e_1, e_2, e_3, \ldots, e_k\}$ (Figure 12(d));
5. faces incident to an edge, $e \longmapsto F(e) = \{f_1, f_2\}$ (Figure 12(e));
6. vertices incident to an edge, $e \longmapsto V(e) = \{v_1, v_2\}$ (Figure 12(f)).

For convenience we also define the following *secondary neighbor relations* and associated averaging operators (Figure 13):

1. flaps of a face, $f \longmapsto F^{\triangleright}(f) = \{F \circ E(f)\} \setminus \{f\} = \{f_1, f_2, f_3, \ldots, f_l\}$ (Figure 13(a));
2. 1-ring of a vertex, $v \longmapsto V^{\circlearrowleft}(v) = \{V \circ F(v)\} \setminus \{v\} = \{v_1, v_2, v_3, \ldots, v_k\}$ (Figure 13(b));
3. e-diamond of an edge, $e \longmapsto E^{\diamondsuit}(e) = \{E \circ F(e)\} \setminus \{e\} = \{e_1, e_2, e_3, e_4\}$ (Figure 13(c));
4. v-diamond of an edge, $e \longmapsto V^{\diamondsuit}(e) = V \circ F(e) = \{v_1, v_2, v_3, v_4\}$ (Figure 13(d)).

(Note that we restricted the last two rules to the triangle case though they may be defined equally well for arbitrary polygons.) This list could be continued but the above relations are sufficient for our purposes.

Each of the above neighbor relations automatically defines an associated *geometric (averaging) rule* if we follow the scheme

$$x \longmapsto Y(x) = \{y_1, \ldots, y_m\} \quad \longrightarrow \quad g(x) = \frac{1}{m} \sum_{l=1}^{m} h(y_l) \ ,$$

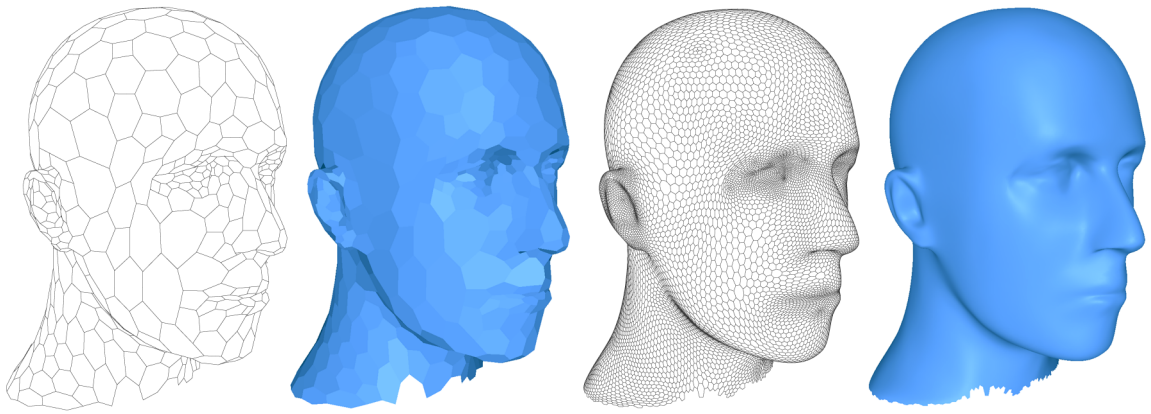


Figure 10: *Dual control mesh and surface after* 4 *levels of* $FVF(2)$ *with weight modification for* $k = 3, 4$.

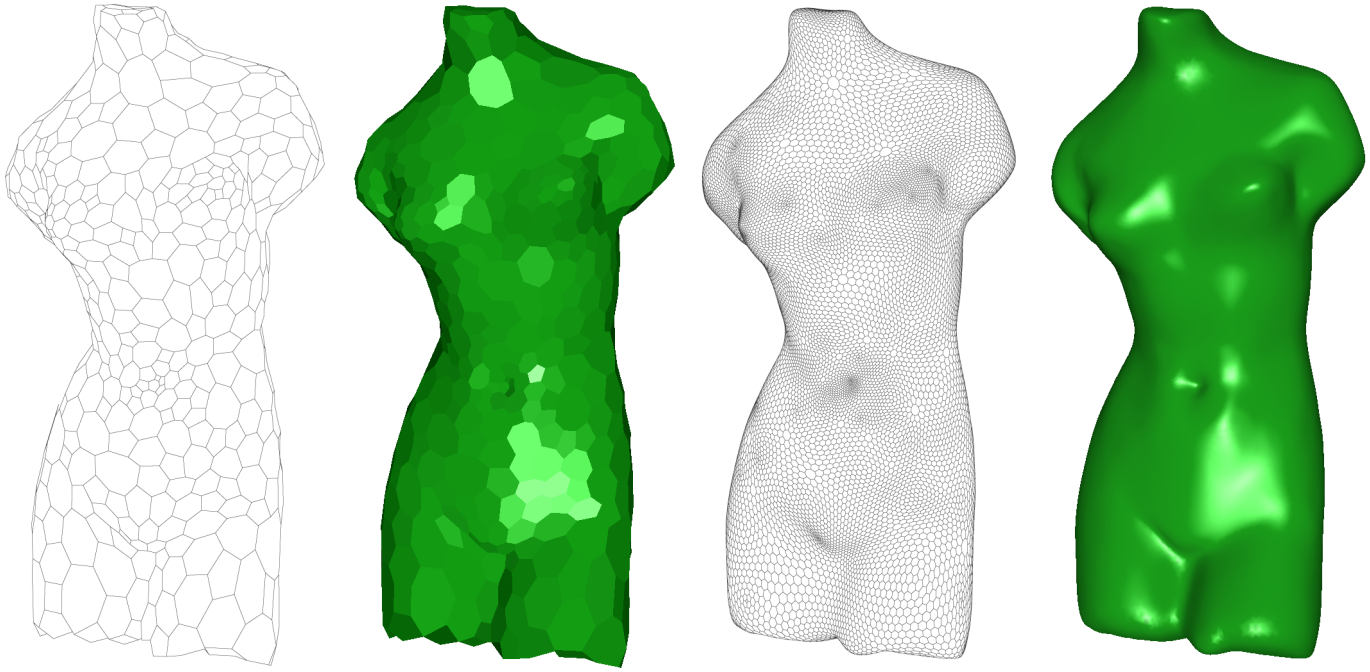
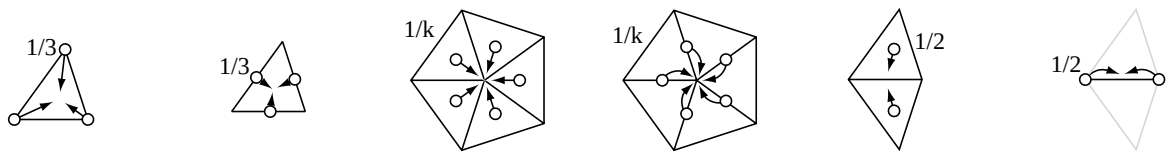


Figure 11: *Dual control mesh and surface after* 4 *levels of* $FVF(2)$ *with weight modification for* $k = 3, 4$.

where h is a discrete function defined on topologic elements of type $Y = V, E,$ or F (mapping into $\mathbb{R}^n$) while the result g is another such function for type X topologic elements. We denote such an averaging rule by YX (since it maps Y-values into X-values). For example, our earlier FV and VF rules followed this convention. For the neighbor relations introduced above the associated averaging rules are given in Figures 12 and 13 for the triangle case ($l = 3$).

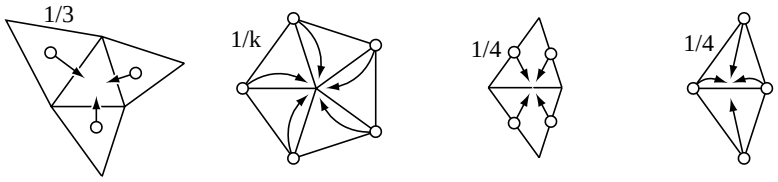
Figure 14 (a-c) depicts some natural parametric generalizations of the averaging rules VV, FF, and $E^{\diamondsuit}E$ which are built by affine combination of these rules with the identity map for the corresponding topologic quantity. By restricting the parameter to $0 \leq c \leq 1$, i.e., by taking convex combinations only, the non-negativity of all coefficients involved will be ensured. More precisely, VV_c uses c-times the identity $g(v) = h(v)$ and $(1 - c)$-times the averaging rule VV. Similarly FF_c employs the identity on f and the averaging rule FF, and $E^{\diamondsuit}E_c$ uses the identity on e and the averaging rule for $E^{\diamondsuit}$. Note that FV_c defined earlier follows as the composition of $FV \circ FF_{3c-2}$. In Figure 14(d), we also define a parametric rule $V^{\diamondsuit}E_c$ by affine combination of $V^{\diamondsuit}E$ and VE.

Although we do not intend to use all rules, having them at our disposal gives us enough flexibility to define a large number of *composite rules*. Coupling them with simple upsampling procedures gives a wide variety of *composite subdivision schemes*. More generally, one step of a composite subdivision operator S is defined by a finite number of averaging rules applied on the coarse mesh, a trivial subdivision step T_{XY} which transforms X-values on the coarse mesh into Y-values on the fine mesh, followed by another set of averaging rules applied on the fine mesh. The only condition is topologic compatibility of the substeps, i.e., an XY-rule should be followed by a YZ-rule, and so on. In most of the cases, we use trivial upsampling $T_{VV,r}$



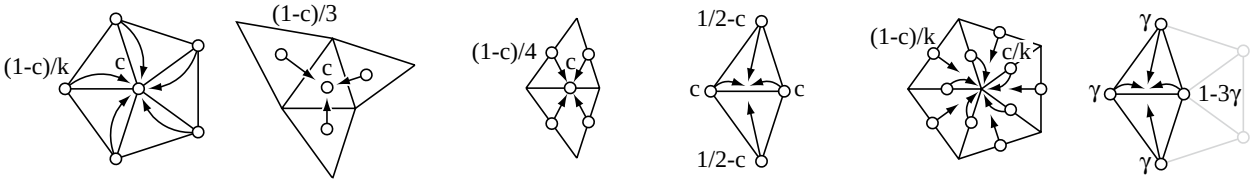
(a) VF rule. (b) EF rule. (c) FV rule. (d) EV rule. (e) FE rule. (f) VE rule.

Figure 12: *Averaging rules associated with the* primary *neighbor relations illustrated in the case of triangles.*



(a) FF rule. (b) VV rule. (c) $E^{\diamond}E$ rule. (d) $V^{\diamond}E$ rule.

Figure 13: *Averaging rules associated with the* secondary *neighbor relations illustrated in the case of triangles.*



(a) VV_c rule. (b) FF_c rule. (c) $E^{\diamond}E_c$ rule. (d) $V^{\diamond}E_c$ rule. (e) EV_c rule. (f) $\widetilde{V^{\diamond}E}_{\gamma}$ rule.

Figure 14: *Parametric generalizations of some averaging rules. Note that (e) is a flap style modification of EV while (f) belongs to the class of weight modifications (for $V^{\diamond}E$).*

where the vertex values associated with the coarse mesh are multiplied by r and copied to the old vertices in the refined mesh, while zero values are assigned to the new vertices. Different topologic refinement results in different values of r, e.g., we have $r = 3$ for $\sqrt{3}$-refinement, and $r = 4$ for quadrisection. Other choices for T_{XY} will be discussed later. Throughout the further discussion, we will only consider *stationary schemes*. For these the set and the order of components used in the definition of the composite scheme are not changed from subdivision step to subdivision step.

In the following, we give examples that demonstrate the potential advantages and the flexibility of building schemes through averaging rules. We start with topologic $\sqrt{3}$-subdivision:

- $S = (FV \circ VF)^n \circ T_{VV,3}$ are the $VFV(n)$ schemes.
- $S = FV \circ FF \circ VF \circ T_{VV,3}$ is Kobbelt's approximating scheme. It turns out that the scheme is automatically C^1 for all valences $k > 3$, and that replacing the FV rule by FV_c with $c < 1$, or FF by some suitable weight modification $\widetilde{FF}_{\beta}$, will again remove the problem for $k = 3$ (for the analysis see Appendix A.5). Kobbelt's original choice follows as $c = 2(\cos(2\pi/k) + 1)/3$. As a by-product we see that the dual scheme $S = FF \circ VF \circ T_{VV,3} \circ FV$ inherits the properties of Kobbelt's scheme.
- $S = T_{FV} \circ FF_c \circ VF$ with a more complex face to vertex upsampling operator T_{FV} which assigns values at the new vertices in the finer mesh as flap averages FF *from the coarser mesh* and values at the old vertices in the finer mesh as face centroids FV *from the coarser mesh*. The resulting one-parameter family of $\sqrt{3}$-subdivision schemes gives highly smooth surfaces in the regular setting. E.g., if $c = 1$ where the identity map FF_1 can be omitted, we get the six-directional C^3 boxspline associated with $\sqrt{3}$-subdivision, with Sobolev smoothness 4.5 and Hölder smoothness < 4. Another remarkable special

case is $c = 0$, where $FF_c = FF$ and the Sobolev smoothness exponent becomes ≈ 5.9402. For $c = 1/3$, the Sobolev smoothness becomes even higher (≈ 6.9087).

This list could be continued. Note that the above schemes use only averaging rules associated with the neighbor relations $V(f)$, $F(v)$, $F^{\triangleright}(f)$. In particular, no edge elements are involved. This situation changes for dyadic subdivision, where the refinement is associated with edge midpoint insertion. In particular, the most appealing primal schemes cannot be obtained by using only V and F elements.

- $S = VEV(n) = (EV \circ V^{\diamondsuit}E)^n \circ T_{VV,4}$ corresponds in the regular case to the family of 3-direction boxsplines of degree $3n - 2$ (see also [12]). In particular, $n = 1$ gives piecewise linear C^0-spline surfaces and $n = 2$ is Loop's scheme [9] (using the irregular vertex weights proposed by Warren [15]). We will call these schemes $VEV(n)$, thereby expressing their similarity to $VFV(n)$. For irregular vertices of valence $k > 3$, this implementation of the Loop scheme is automatically C^1. As in the case of VFV we propose two choices to recover the C^1 property for $k = 3$: a flap and a weight modification. The former replaces EV by EV_c, the analogon of the flap rules for edges (Figure 14(e)). The latter replaces $V^{\diamondsuit}E$ with its weighted version $\widetilde{V^{\diamondsuit}E}_\gamma$ (Figure 14(f)). In Appendix A.6 we show that any $0 \leq c < 1$ or $0 \leq \gamma < 1/4$ are suitable. Negative values are also feasible. Classical choices, such as Warren's for $k = 3$ are recovered with $c = -1/2$, while Loop's (for all k) follows with $c = (3/2 + \cos(2\pi/k))^2/2 - 1$.
- For quadrisection, dual schemes are still equivalent to face-to-face subdivision, thus, there is no easy way to extract a dual scheme from the above $VEV(n)$. To create a hierarchy of such dual schemes for the case of quadrisection, we propose the primal schemes $VFFV(n)$ defined by
$$S = (FV \circ FF_{1/4} \circ VF)^n \circ T_{VV,4} \ ,$$
which involve $FF_{1/4}$ in addition to the elementary averaging rules already used for $VFV(n)$. The properties of $VFFV(n)$ are surprisingly close to those of $VFV(n)$ for both the regular and irregular vertex case (see Appendix A.7 for more details). Having introduced $VFFV(n)$, an associated family $FVFF(n)$ of dual schemes inheriting the properties of $VFFV(n)$ is given by
$$S = FF_{1/4} \circ VF \circ VFFV(n-1) \circ FV \ .$$
- One can directly create the dual subdivision scheme associated with the cubic C^1 half-box splines [10] by averaging
$$S = FF_{1/4} \circ FF_{-1/2} \circ FF_{1/4} \circ T_{FF,4} = FF_{-1/2} \circ FF_{1/4} \circ FF_{1/4} \circ T_{FF,4} = FF_{1/4} \circ FF_{1/4} \circ FF_{-1/2} \circ T_{FF,4} \ .$$
Here, $T_{FF,4}$ is a trivial dual upsampling procedure, where the value associated with a coarse triangle is multiplied by four and written to its center child. All other faces at the finer level receive zero assignments. The order in which the averaging rules $FF_{1/4}$ and $FF_{-1/2}$ are applied does not matter (this is not the case for any other of the above composite rules!). The smoothness near irregular vertices, and the proposed modifications for low-valence vertices are investigated in Appendix A.8.

4 Conclusion

In this paper we explored the construction of primal and dual $\sqrt{3}$-subdivision schemes through application of repeated averaging operators. These are exceptionally simple and build increasing ladders of primal/dual subdivision schemes mimicking a similar setup known from the quadrilateral setting. Smoothness problems typically appear for low valence vertices, and in particular valence $k = 3$. These can be alleviated through parameterized versions of the elementary averaging operators (flap and weight modifications).

Taking into account all topologic quantities, i.e., vertices, edges and faces, we then considered averaging operators which mix these quantities and give rise to an even broader set of constructions which contain many well known examples from primal/dual trisection/quadrisection of triangle meshes. These constructions contain both new and old schemes. For known schemes this recasting in terms of repeated averaging steps results in new insights regarding the construction of dual schemes, for example.

The initial explorations undertaken here pose a number of questions which we leave for future investigation:

- Is there a comprehensive treatment of the question of smoothness near irregular vertices resp. faces, which can leverage the composite nature of the schemes? Perhaps for repeated averaging schemes using only non-negative weights simple sufficient conditions are possible?
- Can one take advantage of the product structure of the subdivision operator S when analyzing $\tilde{S}$ as is the case in the regular setting?
- Is there a theorem saying "$XYZ...X(n+1)$ has smoothness properties as least as good as $XYZ...X(n)$"?
- Is there a natural example of composite schemes based on repeated averaging (with non-negative weights) where not only $k = 3$ but also $k = 4$ or $k = 5$ or k large would cause trouble?

Acknowledgements The work of the second author was supported in part by NSF (DMS-9874082, ACI-9721349, DMS-9872890, ACI-9982273), Lucent, Intel, Alias|Wavefront, Pixar, Microsoft, and the Packard Foundation.

References

[1] CATMULL, E., AND CLARK, J. Recursively Generated B-Spline Surfaces on Arbitrary Topological Meshes. *Computer Aided Design 10*, 6 (1978), 350–355.

[2] DOO, D., AND SABIN, M. Analysis of the Behaviour of Recursive Division Surfaces near Extraordinary Points. *Computer Aided Design 10*, 6 (1978), 356–360.

[3] GUSKOV, I. *Irregular Subdivision and its Applications*. PhD thesis, Princeton University, 1999.

[4] JIANG, Q., AND OSWALD, P. On the Analysis of $\sqrt{3}$-Subdivision Schemes. Submitted for publication, April 2001.

[5] JIANG, Q., OSWALD, P., AND RIEMENSCHNEIDER, S. $\sqrt{3}$-Subdivision Schemes: Maximal Sum Order Rules. Submitted for publication, August 2001.

[6] KOBBELT, L. $\sqrt{3}$ Subdivision. *Proceedings of SIGGRAPH 2000* (July 2000), 103–112.

[7] LABSIK, U., AND GREINER, G. Interpolatory $\sqrt{3}$-Subdivision. *Computer Graphics Forum 19*, 3 (August 2000), 131–138.

[8] LANE, J., AND RIESENFELD, R. A Theoretical Development for the Computer Generation and Display of Piecewise Polynomial Surfaces. *IEEE Trans. Pattern Analysis Machine Intell. 2*, 1 (1980), 35–46.

[9] LOOP, C. Smooth Subdivision Surfaces Based on Triangles. Master's thesis, University of Utah, Department of Mathematics, 1987.

[10] PRAUTZSCH, H., AND BOEHM, W. *The Handbook of Computer Aided Geometric Design*. Elsevier, 2000, ch. Box Splines.

[11] REIF, U. A Unified Approach to Subdivision Algorithms near Extraordinary Points. *Comput. Aided Geom. Des. 12* (1995), 153–174.

[12] STAM, J. On Subdivision Schemes Generalizing Uniform B-Spline Surfaces of Arbitrary Degree. *Comput. Aided Geom. Des. 18*, 5 (June 2001), 383–396.

[13] UMLAUF, G. Analyzing the Characteristic Map of Triangular Subdivision Surfaces. *Constructive Approximation 16*, 1 (2000), 145–155.

[14] VELHO, L. Quasi 4-8 Subdivision. *Comput. Aided Geom. Des. 18*, 4 (2001), 345–357.

[15] WARREN, J. Subdivision Methods for Geometric Design. Unpublished manuscript, November 1995.

[16] ZORIN, D. A Method for Analysis of C^1-Continuity of Subdivision Surfaces. *SIAM J. Numer. Anal. 37*, 5 (2000), 1677–1708.

[17] ZORIN, D., AND SCHRÖDER, P. A Unified Framework for Primal/Dual Quadrilateral Subdivision Schemes. *Comput. Aided Geom. Des. 18*, 5 (June 2001), 429–454.

A Appendices

Our main aim here is to verify the conditions for the existence of a dominant pair of eigen spaces for our schemes by studying the block-diagonal form of the linear subdivision operator $\tilde{S}$ for the invariant neighborhood of the irregular point (vertex or face). The properties of the associated characteristic map are evaluated numerically. A rigorous treatment of its regularity and injectivity properties along the lines of [16] is beyond the scope of this paper.

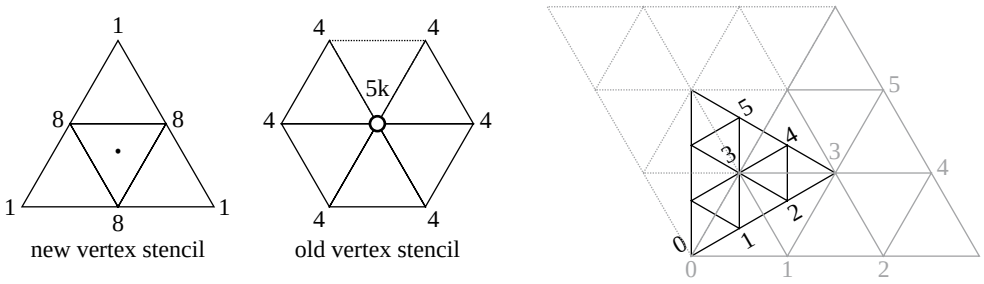


Figure 15: *Stencils for old and new vertices for $VFV(2)$ where k denotes the valence of the center vertex. On the right a section of the invariant neighborhood with the unique vertices relevant for $VFV(2)$ numbered.*

A.1 Details for $VFV(2)$

Figure 15 shows a portion (solid gray) of a k-regular triangulation around an irregular vertex 0 at the coarser level and the image of a fixed reference wedge of this triangulation under subdivision on the next finer level (solid black). The invariant neighborhood for $VFV(2)$ consists of $1+5k$ points: the irregular vertex 0, the points with numbers $1,\ldots,5$ in the reference wedge, together with their copies to the other $k-1$ wedges. The reader may easily check that the restriction of the limit subdivision surface to a certain neighborhood of the irregular vertex, namely to the triangles in the 1-ring U_1' after the first refinement step, only depends on the control points associated with the vertices in the above invariant neighborhood. Using the vertex numbering from the figure and powers of z to indicate the wedge numbering clockwise around the irregular vertex, the subdivision matrix can be written in the Fourier domain in block-diagonal form. Let

$$\tilde{B}(z) = \frac{1}{27}\begin{pmatrix} 15 & 12 & 0 & 0 & 0 & 0 \\ 8 & z^{-1}+8+8z+z^2 & 0 & 1 & 0 & 0 \\ 1 & 8+8z & 1+z & 8 & 0 & 0 \\ 2 & 2+15z+2z^2 & 2z & 2+2z & 0 & 0 \\ 0 & 1+8z & 8z & 8+z & 0 & 1 \\ 0 & 8z+z^2 & 8z & 1+8z & z & 0 \end{pmatrix}, \qquad z = e^{it},$$

and denote by $B(z)$ the 5×5 submatrix obtained by deleting the first column and row from $\tilde{B}(z)$. Then $\tilde{S}$ is similar to the block-diagonal matrix $\mathrm{diag}(B_0, B_1, \ldots, B_{k-1})$, where $B_0 := \tilde{B}(1)$ and $B_j := B(\omega_k^j)$, $j = 1,\ldots,k-1$ ($\omega_k := e^{i2\pi/k}$). The similarity transform is given by an appropriately scaled block-DFT matrix followed by a permutation (see [16, Eq. (2.6)]) and is thus unitary up to a diagonal scaling. The coefficients for the polynomial entries of $\tilde{B}(z)$ can be computed easily by using the stencils shown in Figure 15.

Thus, in order to investigate the spectrum of $\tilde{S}$, we have to assess the spectra of $\tilde{B}(1)$ and $B(z)$ evaluated at the k-th roots of unity. Due to the 4×2 zero submatrix in the last two columns of $\tilde{B}(1)$ resp. $B(z)$, we always have the eigen values

$$\tilde{\lambda}_{5..6} = \pm\frac{1}{27} \quad \text{resp.} \quad \lambda_{4..5}(e^{it}) = \pm\frac{e^{it/2}}{27},$$

and are left with eigen value problems for the smaller matrices

$$\tilde{B}'(1) = \frac{1}{27}\begin{pmatrix} 15 & 12 & 0 & 0 \\ 8 & 18 & 0 & 1 \\ 1 & 16 & 2 & 8 \\ 2 & 19 & 2 & 4 \end{pmatrix}, \qquad B'(z) = \frac{1}{27}\begin{pmatrix} z^{-1}+8+8z+z^2 & 0 & 1 \\ 8+8z & 1+z & 8 \\ 2+15z+2z^2 & 2z & 2+2z \end{pmatrix}.$$

Using Maple, we find the eigen values

$$\tilde{\lambda}_1 = 1, \quad \tilde{\lambda}_2 = \frac{1}{3}, \quad \tilde{\lambda}_{3..4} = \frac{3\pm\sqrt{33}}{54},$$

for $\tilde{B}'(1)$. Thus, the subdominant eigen value of B_0 is $1/3$, independently of k.

The eigen values of $B'(e^{it})$ are simple and of the form

$$\lambda_r(e^{it}) = e^{it/2}\rho_r(t), \quad r = 1,2,3,$$

where the functions $\rho_r(t)$ are real-valued. Indeed, setting $\hat{x} = \mathrm{diag}(z^{1/2}, z^{1/2}, 1)x$ and $\hat{\lambda} = z^{-1/2}\lambda$ one easily computes that

$$B'(z)x = \lambda x \qquad \Longleftrightarrow \qquad \hat{B}(z)\hat{x} = \hat{\lambda}\hat{x} \ ,$$

where

$$\hat{B}(z) = \frac{1}{27}\begin{pmatrix} \frac{1}{z\sqrt{z}} + 8\frac{1}{\sqrt{z}} + 8\sqrt{z} + z\sqrt{z} & 0 & 1 \\ 8(\frac{1}{\sqrt{z}} + \sqrt{z}) & \frac{1}{\sqrt{z}} + \sqrt{z} & 8 \\ \frac{2}{z} + 15 + 2z & 2 & 2(\frac{1}{\sqrt{z}} + \sqrt{z}) \end{pmatrix} = \frac{1}{27}\begin{pmatrix} 2\cos\frac{t}{2}(7 + 2\cos t) & 0 & 1 \\ 16\cos\frac{t}{2} & 2\cos\frac{t}{2} & 8 \\ 15 + 4\cos t & 2 & 4\cos\frac{t}{2} \end{pmatrix}$$

is real-valued and has three distinct real eigen values for all t. The function

$$\rho(t) = \max_r |\rho_r(t)| = \max_r |\lambda_r(e^{it})|$$

satisfies $\rho(2\pi - t) = \rho(t)$ and is strictly monotonically decreasing on $[0, \pi]$, with $\rho(0) \approx 0.719822$, $\rho(2\pi/3) = 1/3$, $\rho(\pi) = 1/(3\sqrt{3})$. As a consequence, there are two dominant (complex conjugate) eigen values for the matrices B_j, one associated with B_1, the other with B_{k-1}. Their absolute value is always $> 1/3$, except for the case $k = 3$. These facts are illustrated in the first two graphs of Figure 16.

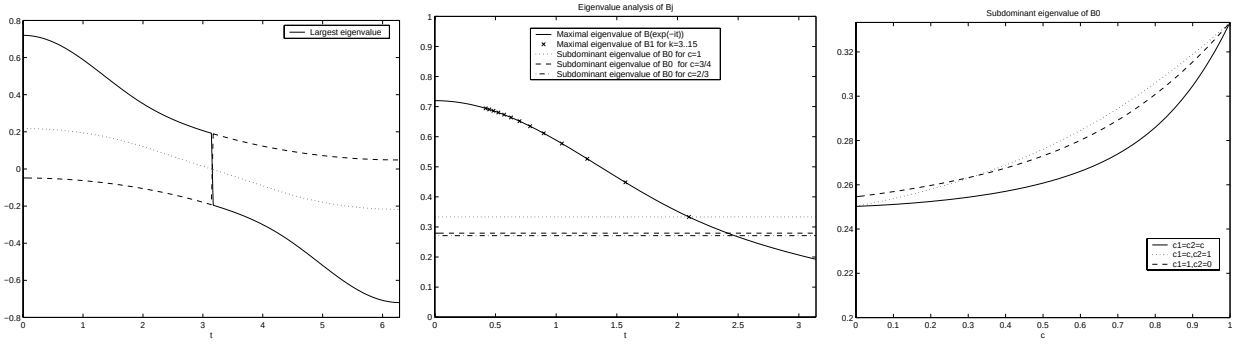


Figure 16: *Numerical data on the spectra of $B'(e^{it})$ and $\tilde{B}'(1)$.*

Altogether, we see that except for $k = 3$, we can determine a unique pair

$$\lambda_2 = \lambda_1(e^{i2\pi/k}) \ , \qquad \lambda_3 = \lambda_1(e^{i2\pi(k-1)/k}) \qquad (|\lambda_2| = |\lambda_3|)$$

of subdominant complex conjugate eigen values of $\tilde{S}$ (i.e., satisfying $1 > |\lambda_2| = |\lambda_3| > |\lambda_4| \geq \ldots$). The same property holds for $VFV(3)$. For $k = 3$, a dominant pair of eigen spaces cannot exist since we have $|\lambda_2| = |\lambda_3| = \lambda_4 = 1/3$. This stalls the further investigation in this case.

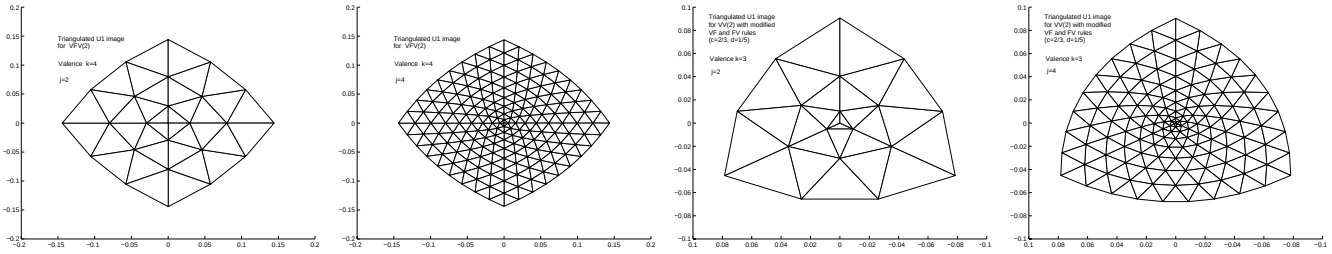


Figure 17: *Visualization of the characteristic map for $VFV(2)$ for valence $k = 4$ (on the left), and the modified $VFV(2)$ for valence $k = 3$ (on the right).*

For $k \geq 4$, the characteristic map Φ is defined by applying subdivision to the real and imaginary part of the eigen vector corresponding to $\lambda_2 = \lambda_1'(e^{jt})$, and restricting the limiting function to the triangles in the 1-ring neighborhood U_1 of 0. Thus, we can view the characteristic map as the result of applying the subdivision scheme to a given (compactly supported) set $\{(f_1^0, f_2^0)\}$ of two-dimensional control points associated with the vertices of the k-regular triangulation around 0. Approximately, the regularity and injectivity of this map can be judged from the triangulation obtained from the control points $\{(f_1^j, f_2^j)\}$ after some j steps. The first two pictures of Figure 17 show these triangulations (more precisely, the part corresponding to U_1) after $j = 2, 4$

steps for $k = 4$. Since by definition of the invariant neighborhood and the eigen vectors f_1, f_2 in the definition of the characteristic map these triangulations are similar in the vicinity of the irregular vertex, problems with the characteristic map can usually be spotted already for $j = 0$. For this reason, and the obvious rotational symmetry, we need to show only one wedge of the triangulated image for $j = 0$. For better comparison, especially to better visualize the behavior of the characteristic map as $k \to \infty$, we will map this wedge of angle $2\pi/k$ to a normalized wedge of angle $\pi/2$ resulting in a *normalized characteristic wedge*. Figure 18 shows normalized characteristic wedges for $VFV(2)$ resp. $VFV(3)$ and various k. Obviously, there are no problems in the limit $k \to \infty$.

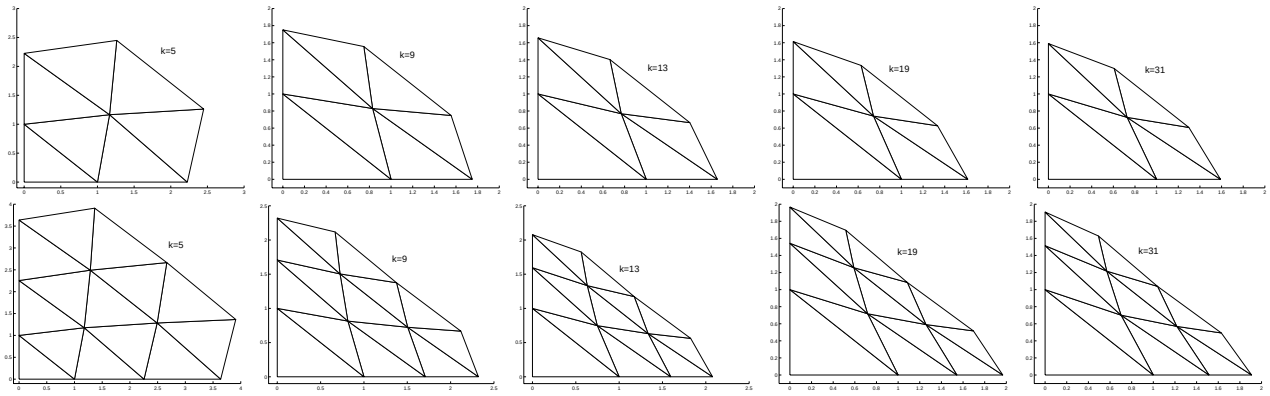


Figure 18: *Normalized characteristic wedges for $VFV(2)$ and $VFV(3)$.*

A.2 Details for Flap Modification

To analyze the effect of these modifications, we consider the operator $\tilde{S}$ for the most general $VFV(2)$-replacement, i.e., for $VFV_{c_1,c_2} = VFV_{c_2} \circ VFV_{c_1} \circ T_{VV,3}$. The stencils for this scheme are shown in Figures 19(a) and 19(b). Note that for $c_1 \neq 1$ we have two types of stencils for new vertices, for those in the 1-ring U_1 of the irregular vertex and for all others. It turns out that the invariant neighborhood for defining $\tilde{S}$ remains the same. Computing the counterpart of $\tilde{B}(z)$ leads us to

$$\tilde{B}(z) = \frac{1}{27} \begin{pmatrix} 6 + 9c_1c_2 & (21 - 9c_1c_2) & 0 & 0 & 0 & 0 \\ (3c_1 + 5) & z^{-1} + 8 + 8z + z^2 + 3(1 - c_1)\delta(z) & 0 & 1 & 0 & 0 \\ 1 & 8 + 8z & 1 + z & 8 & 0 & 0 \\ 2 & 2 + 15z + 2z^2 & 2z & 2 + 2z & 0 & 0 \\ 0 & 1 + 8z & 8z & 8 + z & 0 & 1 \\ 0 & 8z + z^2 & 8z & 1 + 8z & z & 0 \end{pmatrix},$$

where $\delta(z) = (\sum_{l=0}^{k-1} z^l)/k$, i.e., $\delta(\omega_k^j) = \delta_j$, $j = 0, \ldots, k-1$. $B(z)$ and B_j, $j = 0, \ldots, k-1$, are defined as before. Obviously, this implies that the diagonal blocks B_j for VFV_{c_1,c_2} do not depend on the choice of these parameters, and are therefore the same as for $VFV(2)$, where $c_1 = c_2 = 1$. However, the matrix B_0 changes, and in light of our findings for $VFV(2)$ our goal is to decrease its subdominant eigen value $\tilde{\lambda}_2$ below $1/3$. According to our calculations, *any* choice $0 \leq c_1, c_2 \leq 1$, $(c_1, c_2) \neq (1, 1)$ leads to this goal, and to the existence of a dominant pair of eigen spaces. See the third graph in Figure 16 for the behavior of the absolute value $|\tilde{\lambda}_2|$ of the subdominant eigen value of B_0 for the cases of modified $VFV_c(2)$, $VFV_{c,1}(2)$, and $VFV_{c,2}(2)$ schemes and $0 \leq c \leq 1$.

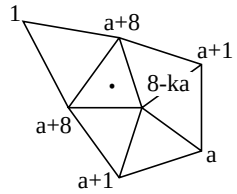
We add a comment which applies to the material in later appendices as well. By restricting our above discussion to non-negative values of c_1, c_2, we guarantee the non-negativity of all coefficients of the averaging rules in *all* substeps of the composite scheme. On the other hand, this restricts our flexibility of influencing the spectrum of $\tilde{S}$. In the above example, the subdominant eigen value of B_0 can be changed into any value in the interval $[1/4, 1/3]$ but not be made smaller than $1/4$ in magnitude. For $k = 3$, the desirable value would be $|\lambda_{2..3}|^2 = 1/9$, which can only be achieved by allowing negative values of c_1.

A.3 Details for Weight Modification

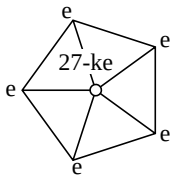
Recall that we defined the $\widetilde{VF}_\alpha$-rule for triangles with one irregular vertex (at v_1) by setting the values of its weights to

$$a_1 = \alpha\ , \quad a_2 = a_3 = (1 - \alpha)/2\ , .$$

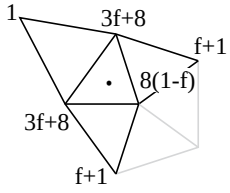
In analogy to the above, we could define modified rules such as $VFV_\alpha(n)$ etc. by replacing VF by $\widetilde{VF}_\alpha$ accordingly. As before, we concentrate on $n = 2$, and consider the general VFV_{α_1,α_2} scheme. To obtain meaningful results, we must have $\alpha_1 = 1/3$,



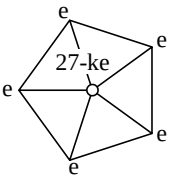
(a) Flap modified stencil near irregular vertex ($a = 3(1 - c_1)/k$).



(b) Flap modified stencil at irregular vertex ($e = (21 - 9c_1c_2)/k$).



(c) Weight modified stencil near irregular vertex ($f = (1 - 3\alpha_2)/4$).



(d) Weight modified stencil at irregular vertex ($e = 18(1 - \alpha_2)/k$).

Figure 19: *Modified $VFV(2)$ scheme stencils for flap and weight modifications (standard stencils are shown in Figure 15).*

which rules out the use of $VFV_{\alpha,1}(n)$ and $VFV_{\alpha}(n)$. Otherwise, constants are not preserved by the scheme VFV_{α_1,α_2}, and the leading eigen value of $\tilde{S}$ has value $\neq 1$ which violates the convergence condition of the subdivision scheme at the irregular vertex.

After setting $\alpha_1 = 1/3$ and $\xi = (1 - 3\alpha_2)/4$, we derive the stencils shown in Figures 19(c) and 19(d), and obtain the counterpart of $\tilde{B}(z)$ as

$$\tilde{B}(z) = \frac{1}{27}\begin{pmatrix} 15-24\xi & 12+24\xi & 0 & 0 & 0 & 0 \\ 8-8\xi & ((1+\xi)(z^{-1}+z^2)+(8+3\xi)(1+z) & 0 & 1 & 0 & 0 \\ 1 & 8+8z & 1+z & 8 & 0 & 0 \\ 2 & 2+15z+2z^2 & 2z & 2+2z & 0 & 0 \\ 0 & 1+8z & 8z & 8+z & 0 & 1 \\ 0 & 8z+z^2 & 8z & 1+8z & z & 0 \end{pmatrix}.$$

This time both the subdominant eigen value of B_0 and the leading eigen values of $B(e^{it})$ resp. $\hat{B}(e^{it})$ will change. Fortunately, if $\xi > 0$ then the subdominant eigen value of B_0 will become less than $1/3$ while the dominant eigen value of $\hat{B}(e^{i2j\pi/k})$ (and thus of B_j) is larger than $1/3$, for all $j = 1, \ldots, k-1$, and $k = 3, 4, 5$.

According to the above, we can recommend the use of the $VFV_{\alpha,n}(n)$ scheme, with the modification $\alpha < 1/3$ switched on only for small k. Although asymptotically it does not matter whether we use the specific weights proposed in Section 2.1.3 for the triangles around an irregular vertex, or any other $\widetilde{VF}_{\alpha}$-rule with parameter $\alpha < 1/3$, the shape of basis functions for vertices of valence $k = 3, 4$ shown in Figure 7 indicate that smaller α-values generally yield better visual results which has its explanation in the decreasing $|\lambda_4|/|\lambda_{2..3}|$ ratio. In analogy to the observations for flap modifications, values $\alpha < 0$ are required to obtain optimal visual performance for valences $k = 3, 4$.

A.4 $FVF(n)$ and Other Dual Schemes

Above we have asserted that dual schemes such as $FVF(n)$ or $FVFF(n)$ inherit their properties from the primal composite subdivision schemes they are derived from. We will substantiate this claim by showing the following: *If a composite primal scheme of the form*

$$S_V := \widehat{FV} \circ \widehat{VF} \circ T_{VV,n}$$

(1) consists of averaging rules $\widehat{FV}, \widehat{VF}$ with locally supported and uniformly bounded stencils; (2) has the property that the upsampling rule $\hat{T}_{VF} := \widehat{VF} \circ T_{VV,r}$ reproduces at least constants; and (3) converges in the C-norm then the associated dual scheme

$$S_F := \widehat{VF} \circ T_{VV,r} \circ \widehat{FV}$$

also converges in C. Moreover, the basis functions ϕ_f associated with faces for the dual scheme are finite linear combinations of the basis functions ϕ_v associated with vertices for the primal scheme (with coefficients solely determined by $\widehat{FV}$). Clearly, this implies that the smoothness properties of the two schemes are essentially the same. In particular, the above result covers $FVF(n)$ if we set

$$\widehat{FV} = FV\ , \quad \widehat{VF} = VF \circ (FV \circ VF)^{n-1}\ , \quad r = 3\ ,$$

the modified rules are obtained by substituting FV by the flap modification resp. VF by the weight modification accordingly. Analogously, in order to treat $FVFF(n)$ we have to set

$$\widehat{FV} = FV\ , \quad \widehat{VF} = FF_{1/4} \circ VF \circ (FV \circ FF_{1/4} \circ VF)^{n-1}\ , \quad r = 4\ ,$$

Note that another dual scheme denoted by $FFVF(n)$ is obtained by setting

$$\widehat{FV} = FV \circ FF_{1/4} \ , \quad \widehat{VF} = VF \circ (FV \circ FF_{1/4} \circ VF)^{n-1} \ , \quad r = 4 \ .$$

Last but not least, the natural dual to Kobbelt's primal scheme would require setting $\widehat{FV} = FV$, $\widehat{VF} = FF \circ VF$, and $r = 3$. Modifications for the irregular vertex treatment are allowed for substitution in the admissible places.

For simplicity, we will give the argument for the above statements for the triangle case and assume that $\widehat{FV}$ coincides with the elementary averaging rule FV. Let $\mathcal{V}_m$, $\mathcal{F}_m$ denote the sets of vertices and faces (triangles) after m refinement steps. Let e_v, e_f be unit coordinate vectors of length $|\mathcal{V}_0|$, $|\mathcal{F}_0|$ associated with $v \in \mathcal{V}_0$, $f \in \mathcal{F}_0$, respectively. By the assumptions on the primal scheme, for each $v \in \mathcal{V}_0$, there exists a unique locally supported continuous basis function ϕ_v such that

$$\varepsilon_v(m) := \max_{\mathcal{V}_m} |S_V^m e_v - \phi_v|_{\mathcal{V}_m}| \ \longrightarrow \ 0 \ , \qquad m \ \longrightarrow \ \infty \ .$$

Set $\phi_f := (\sum_{v \in f} \phi_v)/3$ for each $f \in \mathcal{F}_m$, and consider

$$\varepsilon_f(m) := \max_{\mathcal{F}_m} |S_F^m e_f - \phi_f|_{\mathcal{F}_m}| \ .$$

Without loss of generality, the sequence $\phi_f|_{\mathcal{F}_m}$ is defined by assigning the values of ϕ_f at the barycenters to the faces in $\mathcal{F}_m$.

By definition of S_F, we can write

$$S_F^m = \widehat{VF} \circ T_{VV,r} \circ S_V^{m-1} \circ FV \ .$$

Since $FVe_f = (\sum_{v \in f} e_v)/3$, we have the component-wise estimate

$$\begin{aligned} |S_F^m e_f - \phi_f|_{\mathcal{F}_m}| &\leq \frac{1}{3} \sum_{v \in f} |\hat{T}_{VF} \circ S_V^{m-1} e_v - \phi_v|_{\mathcal{F}_m}| \\ &\leq \frac{1}{3} \sum_{v \in f} |\hat{T}_{VF}(S_V^{m-1} e_v - \phi_v|_{\mathcal{V}_{m-1}})| + \frac{1}{3} \sum_{v \in f} |\hat{T}_{VF} \phi_v|_{\mathcal{V}_{m-1}} - \phi_f|_{\mathcal{F}_m})| \\ &\equiv \varepsilon_1 + \varepsilon_2 \ . \end{aligned}$$

Since $\varepsilon_1 \leq C \sum_{v \in f} \varepsilon_v(m-1)$ with C only depending on the coefficients of the upsampling rule $\hat{T}_{VF}$, we have $\varepsilon_1 \to 0$ as $m \to \infty$ (uniformly with respect to $f \in \mathcal{F}_0$). Moreover, since $\hat{T}_{VF}$ is local and preserves constants, and the compactly supported ϕ_v are uniformly continuous, we also have $\varepsilon_2 \to 0$. This proves that $\varepsilon_f(m) \to 0$ for $m \to \infty$. In other words, $S_F^m e_f$ converges uniformly to the continuous function $\phi_f = (\sum_{v \in f} \phi_v)/3$ for any $f \in \mathcal{F}_0$, which also implies the other statements. Obviously, if $\widehat{FV}$ is defined by a more general local rule, the proof remains the same, only the expression of ϕ_f as a linear combination of primal basis functions ϕ_v has to be changed accordingly.

This derivation also shows that in order to keep the dual scheme as local as possible, it is recommended to construct it with a rule $\widehat{FV}$, which is as compact as possible. E.g., $FVFF(n)$ should be preferred over $FFVF(n)$ in this respect. Note that, in contrast to primal schemes such as $VFV(n)$ and $VFFV(n)$ for which the basis functions ϕ_v are linearly independent, the derived dual schemes usually do not have this property. E.g., if $v \in \mathcal{V}_0$ is a vertex of even valence $k = 2k'$ then

$$\phi_{f_1} - \phi_{f_2} + \ldots + \phi_{f_{2k'-1}} - \phi_{f_{2k'}} = 0 \ ,$$

where $f_1, \ldots, f_{2k'}$ are the triangles attached to v in consecutive order.

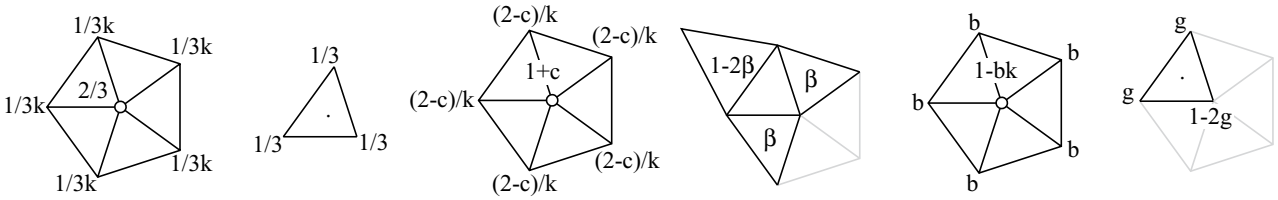
A.5 Details for Kobbelt's scheme

Above, we claimed that in the regular case Kobbelt's scheme can be written as a composite $\sqrt{3}$-subdivision rule, more precisely, as

$$S = FV \circ FF \circ VF \circ T_{VV,3} \ .$$

Figure 20(a) shows the stencils for this S. They coincide with Kobbelt's [6] for $k = 6$. As we will see below, this S guarantees C^1 smoothness for irregular vertices of valence $k > 3$.

To deal with $k = 3$, and to enhance the smoothness properties for low valences $k < 6$, we consider two modifications. First, as we already did for the $VFV(n)$ schemes, we will replace FV by the flap rule FV_c with $c < 1$ resulting in a modified irregular vertex stencil (Figure 20(b)). From the stencils we find that a suitable invariant neighborhood consists of the vertices



(a) Unmodified stencils for Kobbelt's scheme.

(b) Stencil for old vertices when using FV_c modification.

(c) $\widetilde{FF}_\beta$ rule and resulting stencils near irregular vertices ($b = (1-2\beta)/k$, $g = (4-3\beta)/9$).

Figure 20: *Stencils and modifications for Kobbelt's subdivision scheme when expressed through repeated averaging.*

in the 2-ring around the irregular vertex (i.e., generated by the vertices indexed $0, \ldots, 3$ in Figure 15), and compute the matrix functions

$$\tilde{B}(z) = \frac{1}{18}\begin{pmatrix} 6(1+c) & 6(2-c) & 0 & 0 \\ 6 & 6(1+z) & 0 & 0 \\ 0 & 6(1+z) & 0 & 6 \\ 1 & 1+12z+z^2 & z & 1+z \end{pmatrix}, \qquad B(z) = \frac{1}{18}\begin{pmatrix} 6(1+z) & 0 & 0 \\ 6(1+z) & 0 & 6 \\ 1+12z+z^2 & z & 1+z \end{pmatrix}, \qquad z = e^{it}\,.$$

As before, $\tilde{S}$ is similar to $\mathrm{diag}(B_0, B_1, \ldots, B_{k-1})$, where $B_0 = \tilde{B}(1)$ and $B_j = B(\omega_k^j)$, $j = 1, \ldots, k-1$. The 4×4 eigen value problem for B_0 splits into two smaller eigen value problems for the 2×2 diagonal blocks, and we obtain

$$\tilde{\lambda}_1 = 1\,, \quad \tilde{\lambda}_2 = c/3\,, \quad \tilde{\lambda}_{3..4} = (1 \pm \sqrt{7})/18\,.$$

Analogously, the eigen values for $B(e^{it})$ are given by

$$\lambda_1(e^{it}) = \frac{2e^{it/2}}{3}\cos\frac{t}{2}\,, \quad \lambda_{2..3}(e^{it}) = \frac{e^{it/2}}{18}(\cos\frac{t}{2} \pm \sqrt{6+\cos^2\frac{t}{2}})\,.$$

None of these eigen values create nontrivial Jordan blocks. Obviously,

$$|\lambda_{2..3}(e^{it})| \le \frac{1+\sqrt{7}}{18} < \frac{1}{3}$$

for all t, and

$$\max_{j=1,\ldots,k-1} |\lambda_1(2\pi j/k)| = |\lambda_1(2\pi/k)| = 2/3\cos(\pi/k) \ge 1/3\,,$$

for all $k \ge 3$. This maximum is attained in exactly two cases, for $j = 1$ and $j = k-1$. Thus, if we take $c < 1$ then we have a dominant pair of eigen spaces for $\tilde{S}$ associated with B_1 and B_{k-1} since the subdominant eigen value of B_0 becomes smaller than $1/3$. Without this modification, i.e., for $c = 1$, there is a conflict for $k = 3$ since we have a subdominant eigen value $|\lambda_2| = |\lambda_3| = \lambda_4 = 1/3$ of multiplicity 3.

The alternative to using FV_c is to replace the FF rule by its weight modification $\widetilde{FF}_\beta$ as shown in Figure 20(c). Note that the modification is only used if the center triangle of the flap region contains an irregular vertex (with valence $k \ne 6$), in all other cases we use the original FF stencil which is obtained by setting $\beta = 1/3$. The analysis is very similar since the new

$$\tilde{B}(z) = \frac{1}{18}\begin{pmatrix} 36\beta & 18(1-2\beta) & 0 & 0 \\ 12\beta+2 & (8-6\beta)(1+z) & 0 & 0 \\ 0 & 6(1+z) & 0 & 6 \\ 1 & 1+12z+z^2 & z & 1+z \end{pmatrix}, \qquad B(z) = \frac{1}{18}\begin{pmatrix} (8-6\beta)(1+z) & 0 & 0 \\ 6(1+z) & 0 & 6 \\ 1+12z+z^2 & z & 1+z \end{pmatrix}, \qquad z = e^{it}\,.$$

also lead to explicitly solvable eigen value problems. As a result, by choosing $\beta < 1/3$ we achieve

$$\max_{j=1,\ldots,k-1} \max_{r=1,2,3} |\lambda_r(2\pi j/k)| = |\lambda_1(2\pi/k)| = 2(4-3\beta)/9\cos(\pi/k) > 1/3\,,$$

for any $k \ge 3$ while the subdominant eigen value of B_0 becomes $\tilde{\lambda}_2 = (12\beta-1)/9 < 1/3$. This gives a dominating pair of eigen spaces associated with B_1 and B_{k-1} as desired.

Clearly, both modifications may be combined. Note that Kobbelt's original rules [6] would be obtained if we choose the FV_c modification with parameter

$$c = c_k = \frac{4}{3}\cos^2(\pi/k) = \frac{2}{3}(\cos(2\pi/k) + 1) \ ,$$

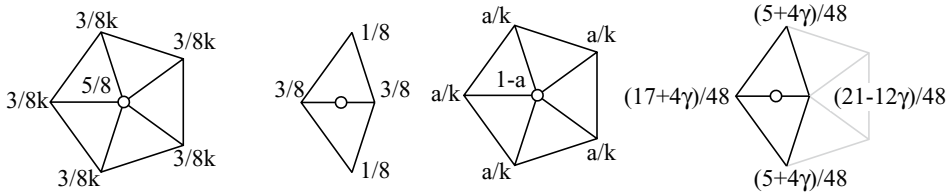
(but leave FF unchanged) in which case the subdominant eigen value of B_0 equals $|\lambda_{2..3}|^2$ as is desirable. Thus, for large k c-values slightly larger than 1 can be used as well.

A.6 Details for Loop's Scheme: $VEV(2)$

The analysis for $VEV(2)$ parallels the one in the previous subsection. We will analyze the following modified $VEV(2)$:

$$S = EV_c \circ \widetilde{V^\diamondsuit E}_\gamma \circ EV \circ V^\diamondsuit E \circ T_{VV,4} = EV_c \circ \widetilde{V^\diamondsuit E}_\gamma \circ VEV(1) \ ,$$

where the flap modification EV_c and the weight modification $\widetilde{V^\diamondsuit E}_\gamma$ were defined in Figures 14(e) and 14(f) and are allowed to have parameter values $c \neq 1$ and $\gamma \neq 1/4$ at irregular vertices only. Obviously, $EV_1 = EV$ and $\widetilde{V^\diamondsuit E}_{1/4} = V^\diamondsuit E$. With these parameters we have Loop's scheme for the regular case. In our analysis below, we will for simplicity assume that the weights in these parameter rules remain non-negative, i.e., $0 \leq c \leq 1$ and $0 \leq \gamma \leq 1/3$. Since $VEV(1)$ is the linear spline subdivision scheme, it is easy to check that the stencils for the above S are as shown in Figure 21.



(a) Unmodified stencils for Loop's scheme.

(b) Stencils for modified Loop scheme near irregular vertices ($a = (1 - (1 - 3\gamma)c)/2$).

Figure 21: *Stencils for Loop's scheme.*

As before, the invariant neighborhood consists of the vertices in the 2-ring around the irregular vertex. From the stencils, we obtain

$$\tilde{B}(z) = \frac{1}{48}\begin{pmatrix} 24(1-c(1-3\gamma)) & 24(1+c(1-3\gamma)) & 0 & 0 \\ 21-12\gamma & 17+4\gamma+(5+4\gamma)(z^{-1}+z) & 0 & 0 \\ 3 & 3(10+z^{-1}+z) & 3 & 3(1+z^{-1}) \\ 6 & 18(1+z) & 0 & 6 \end{pmatrix} \ ,$$

and

$$B(z) = \frac{1}{48}\begin{pmatrix} 17+4\gamma+(5+4\gamma)(z^{-1}+z) & 0 & 0 \\ 3(10+z^{-1}+z) & 3 & 3(1+z^{-1}) \\ 18(1+z) & 0 & 6 \end{pmatrix} \ , \qquad z = e^{it} \ .$$

From this we see that $\tilde{S}$ has eigen values $1/8$ and $1/16$ of multiplicity at least k. The remaining eigen values are

$$\lambda(e^{i2\pi j/k}) = (17 + 4\gamma + 2(5+4\gamma)\cos(2\pi j/k))/48 \ ,$$

and correspond to the matrices B_j, $j = 1, \ldots, k-1$, while B_0 contributes the leading eigen value 1 and

$$\lambda = (1 + 8c(1-3\gamma) + 4\gamma)/16 \ .$$

Since all B_j are similar to diagonal matrices, there are no nontrivial cyclic eigen spaces. To ensure a dominating pair of eigen spaces associated with B_1 and B_{k-1}, the following inequality has to be satisfied:

$$\lambda(e^{i2\pi/k}) = (17 + 4\gamma + 2(5+4\gamma)\cos(2\pi/k))/48 > \max(1/8, (1 + 8c(1-3\gamma) + 4\gamma)/16) \ ,$$

or, equivalently,

$$\cos(2\pi/k)) > \frac{\max(6, 3 + 24c(1-3\gamma) + 12\gamma) - 17 - 4\gamma}{10 + 8\gamma} \ .$$

Property	$n=1$	$n=2$	$n=3$
Sum rule order	2	4	6
Stability	yes	yes	yes
Sobolev regularity	1.6209	3.7946	5.8913
Hölder regularity	0.8480	3.2419	5.4501

Table 2: *Basic properties of $VFFV(n)$, $n \leq 3$, in the regular case.*

For the unmodified scheme, i.e., for $c = 1$, $\gamma = 1/4$, the right-hand side becomes $-1/2$, which excludes $k = 3$. On the other hand, if $\gamma = 1/4$ and $0 \leq c < 1$ resp. if $1/4 < \gamma \leq 1/3$ and $c = 1$, it is easy to check that the right-hand side is less than $-1/2$, in which case the condition holds for all valences $k \geq 3$. A more thorough checking shows that the right-hand side remains $< -1/2$ for all c, γ in the specified ranges, except for $0 \leq \gamma \leq 1/3 - 5/(12(6c-1))$, $3/8 \leq c \leq 1$. Note that this holds also for some values $(c, \gamma) \notin [0,1] \times [0, 1/3]$. A full analysis for $\gamma = 1/4$, including the investigation of the characteristic map, has been given by Umlauf [13] (using direct modifications of the stencil for old vertices).

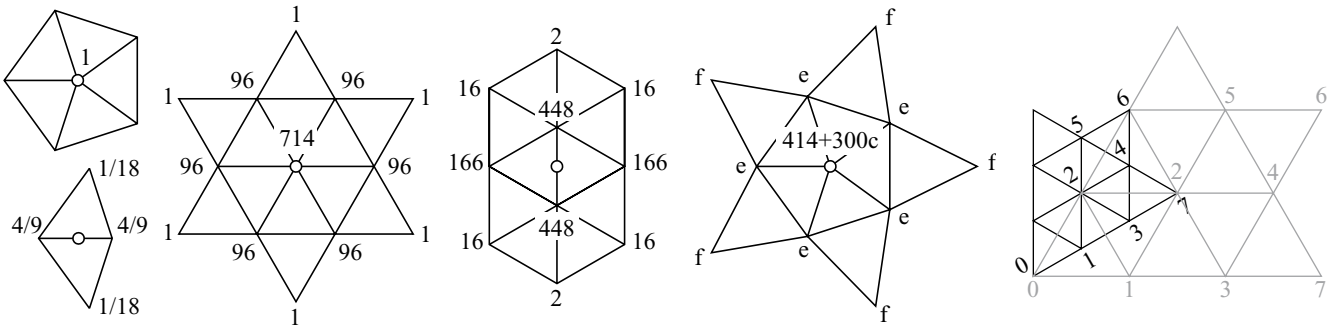
A.7 Details for $VFFV(n)$

These composite primal schemes for the quadrisection case were introduced in Section 3 as a possible counterpart of the $VFV(n)$ schemes. They automatically yield a family of dual schemes with similar properties, see Appendix A.4. Table 2 summarizes the properties of these schemes for the regular case. This analysis is standard (along the lines of [4]) and we omit the details. Increasing n quickly improves both Hölder and Sobolev smoothness.

We will discuss here some details of the irregular vertex treatment for $VFFV(2)$. Since $VFFV(n)$ is the result of repeated application of elementary VF, $FF_{1/4}$, and FV rules, the treatment of potential problems with the smoothness near irregular vertices can be based on replacing the averaging operations VF, FV by the previously proposed modifications $\widetilde{VF}_d$, FV_c, or $FF_{1/4}$ by its weight modification $\widetilde{FF}'_\alpha$ as shown in Figure 24(a). For simplicity, we will only analyze the case of a single FV_c modification with $0 \leq c \leq 1$ in the last step, i.e., we will consider the subdivision scheme

$$S = FV_c \circ FF_{1/4} \circ VF \circ FV \circ FF_{1/4} \circ VF \circ T_{VV,4} \; .$$

Since $VFFV(1)$ is an interpolatory subdivision scheme with stencils as shown in Figure 22(a), the stencils for the above $VFFV(2)$ modification are also easy to derive (Figure 22(b)). A minimal invariant neighborhood suitable for the irregular vertex treatment needs to include $1 + 7k$ vertices (Figure 22(c) shows the corresponding indices in a reference wedge).



(a) Stencils for $VFFV(1)$.

(b) Stencils for modified $VFFV(2)$ scheme for regular vertices (old and new) on the left and at an irregular vertex ($e = (864-288c)/k$, $f = (18-12c)/k$, all coefficients are multiplied by 1296).

(c) Invariant neighborhood labeling for $VFFV(2)$.

Figure 22: *Stencils for $VFFV(1)$ and $VFFV(2)$.*

With this we are in position to generate the associated 8×8 matrix function $\tilde{B}(z)$. To save space, we observe that it contains a 6×2 zero submatrix in the last two columns. Thus, the eigen value problem for $\tilde{S}$ can be reduced to eigen value problems for two smaller matrices. The eigen values of the B_j, $j = 0, \ldots, k-1$, corresponding to the 2×2 submatrix

$$\tilde{B}'(z) = \frac{1}{1296} \begin{pmatrix} 1 & 1+z \\ 0 & 1 \end{pmatrix} \qquad \Longrightarrow \qquad \tilde{\lambda}'_1(z) = \frac{1}{648} \, , \;\; \tilde{\lambda}'_2(z) = \frac{1}{1296} \, ,$$

(with $z = \omega_k^j$) are independent of j, and too small to be of further concern. Thus, we are left with the other 6×6 matrix function

$$\tilde{B}''(z) = \frac{1}{1296} \begin{pmatrix} 414+300c & 864-288c & 18-12c & 0 & 0 & 0 \\ 448 & 448+166(z+z^{-1})+16(z^2+z^{-2})+z^3+z^{-3} & 16(1+z^{-1}) & 2 & 0 & 0 \\ 166 & 448(1+z)+16(z^{-1}+z^2) & 166+2(z+z^{-1}) & 16(1+z) & 0 & 0 \\ 96 & 714+96(z+z^{-1})+(z^2+z^{-2}) & 96(1+z^{-1}) & 96+z+z^{-1} & 1 & z^{-1} \\ 16 & 448+166z+2z^{-1} & 448+16z^{-1} & 166+16z & 16 & 2 \\ 16 & 166+448z+2z^2 & 448+16z & 16+166z & 2 & 16 \end{pmatrix}.$$

The leading eigen values of $B_0'' = \tilde{B}''(1)$ are $\lambda_1'' = 1$ and $\lambda_2'' = 1/4$ if $c = 1$ and $\lambda_2'' < 1/4$ if $0 \le c < 1$. The behavior of λ_2'' as a function of c (Figure 23 (a)) has been investigated numerically. Let $B''(z)$ be the 5×5 submatrix of $\tilde{B}''(z)$ obtained by deleting the first row and column. Note that $B_j'' = B''(e^{i2\pi j/k})$, $j = 1, \ldots, k-1$. These matrices account for the remaining eigen values of $\tilde{S}$. We see from Figure 23 (b) that the largest magnitude eigen values of all B_j come from B_1 and B_{k-1}. Their value is strictly increasing with k, and approaches $0.6653...$ if $k \to \infty$. It is $> 1/4$ for all $k \ge 4$, and $= 1/4$ for $k = 3$. Thus, we can expect the unmodified $VFFV(2)$ scheme ($c = 1$) to yield the C^1 property at irregular vertices, except if we have $k = 3$. To deal with $k = 3$, we should take $c < 1$. The choices $c = 0$ for $k \le 4$, $c \approx 1/2$ for $k = 5$, $c = 1$ for $k \ge 6$ seem to yield a best separation of the subdominant eigen pair $\lambda_{2..3}$ of $\tilde{S}$ from λ_4 within the considered range of non-negative c. As above, further improvements in this respect can only be expected with negative parameter settings.

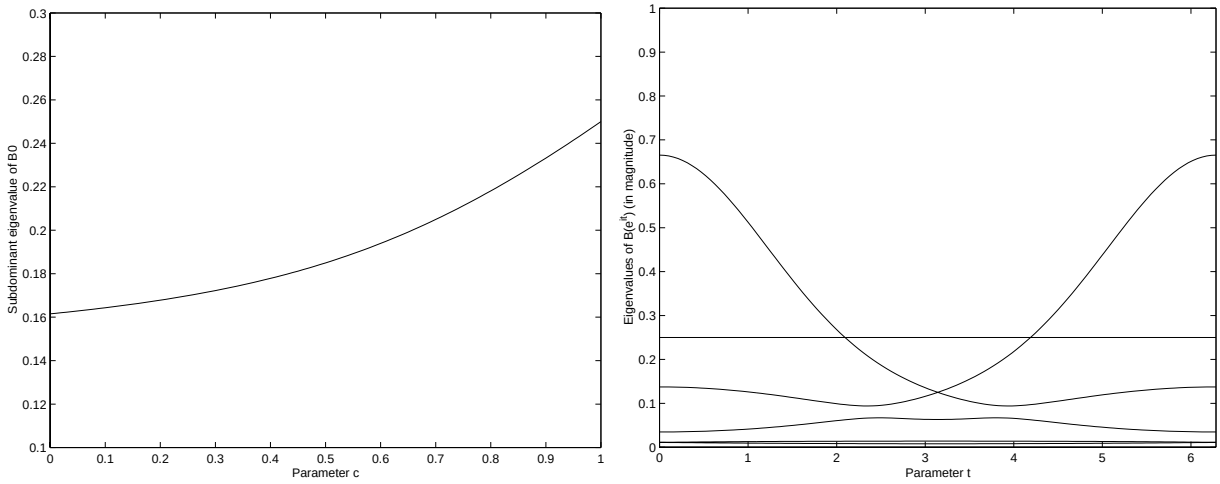


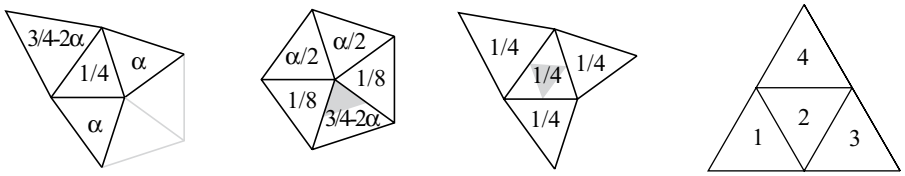
Figure 23: *Subdominant eigen value of B_0 (left) and nontrivial eigen values of $B''(e^{it})$ for $VFFV(2)$ with FV_c modification (right).*

A.8 Details for the Half-Box Spline Scheme

Here we consider the dual subdivision scheme $S = FF_{1/4} \circ FF_{-1/2} \circ FF_{1/4} \circ T_{FF,4}$ for quadrisection. To deal with the C^1 property near irregular vertices of low valence, we replace the $FF_{1/4}$ rule by a weight modification $\widetilde{FF}_\alpha'$ as shown in Figure 24(a). (Note the differences with $\widetilde{FF}_\beta$ used in A.5 which is a weight modification of FF.) Clearly, whenever the irregular vertex is *not* among the vertices of the center triangle we use the original rule $FF_{1/4}$. The stencils for the resulting S are shown in Figure 24(b).

In the regular case, it is well-known that the limiting surface is a C^1 cubic half-box spline with respect to the coarse triangulation. Basis functions are supported in a 1-ring around the face they correspond to. Thus, the 2-ring neighborhood of the irregular vertex can be used as the invariant neighborhood for the subsequent analysis. The enumeration of the faces within this invariant neighborhood is shown in Figure 24(c). After the same scaled unitary transformations as used before we see that $\tilde{S}$ is similar to the block-diagonal matrix $\mathrm{diag}(B_0, B_1, \ldots, B_{k-1})$, where $B_j = B(\omega_k^j)$, $j = 0, \ldots, k-1$, is given by the lower-triangular matrix function

$$B(e^{it}) = \begin{pmatrix} 1-(1-\cos t)/4-\alpha(1-\cos 2t) & 0 & 0 & 0 \\ (1+2\cos t)/4 & 1/4 & 0 & 0 \\ (4+e^{-it})/8 & (1+e^{-it})/8 & 1/8 & 0 \\ (4+e^{it})/8 & (1+e^{it})/8 & 0 & 1/8 \end{pmatrix}.$$



(a) $\widetilde{FF}'_\alpha$ rule.

(b) Resulting stencils (respective child highlighted).

(c) Invariant neighborhood numbering.

Figure 24: *Generalized half-box spline subdivision.*

The eigen values of $\tilde{S}$ are $\lambda = 1/4$ (of multiplicity at least k), $\lambda = 1/8$ (of multiplicity at least $2k$), and

$$\lambda = 1 - (1 - \cos(2\pi j/k))/4 - \alpha(1 - \cos(4\pi j/k)) \ , \qquad j = 0, \ldots, k-1 \ .$$

Thus, in order for $\tilde{S}$ to possess a dominating pair of eigen spaces associated with B_1 and B_{k-1}, we need to ensure that the function $r(t) = 1 - (1 - \cos t)/4 - \alpha(1 - \cos 2t)$ satisfies

$$r(2\pi/k) > \max\{1/4,\, r(2\pi j/k),\, 2 \le j < k/2\} \ .$$

The reason that $j = k/2$ for even k can be excluded is that the corresponding eigen vector of $B_{k/2}$ is $(1 \ -1 \ 1 \ 1)^T$, and leads to a distinguished ± 1 pattern for the associated control net which extends in a natural way to the whole k-regular triangulation. Thus, the limiting surface corresponding to this particular eigen vector of $\tilde{S}$ vanishes in a neighborhood of the irregular vertex, and does not have to be taken into account for the smoothness analysis.

For the half boxspline scheme, i.e., if we take $\alpha = 1/4$, the above condition on $r(t)$ is satisfied if $k \ge 6$ while it is violated for $k < 6$. Indeed, for $k = 3, 4$ the subdominant eigen value is $\lambda = 1/4$ with multiplicity $k + 2$, while for $k = 5$ the subdominant eigen value is $\lambda = 3/8$ with multiplicity 4. Let us verify that taking $\alpha < 1/4$ for $k < 6$ rectifies the situation. We have

$$r(2\pi/5) > r(\pi/2) = 3/4 - 2\alpha > 1/4 \ , \qquad r(2\pi/3) = 1 - 3/2(1/4 + \alpha) > 1/4 \ ,$$

while for $k = 5$ we also have

$$r(2\pi/5) - r(4\pi/5) = (\cos 2\pi/5 - \cos 4\pi/5)(1/4 - \alpha) > 0 \ .$$

This implies the above requirement for all $k < 6$. For practical use, we recommend the following valence-dependent values for $\alpha = \alpha_k$:

$$\alpha_3 = 1/12 \ , \quad \alpha_4 = 1/8 \ , \quad \alpha_5 = 1/4 - 1/(16 \sin^2(2\pi/5)) = 0.1809... \ ,$$

and $\alpha_k = 1/4$ for $k \ge 6$. With these values $\lambda_{2..3} = 1/2$ for $k \le 6$ which separates the subdominant eigen pair sufficiently from the remaining eigen values of S.